



**HAL**  
open science

## Multilevel Algorithms for Acyclic Partitioning of Directed Acyclic Graphs

Julien Herrmann, Yusuf M. Özkaya, Bora Uçar, Kamer Kaya, Ümit V.  
Çatalyürek

► **To cite this version:**

Julien Herrmann, Yusuf M. Özkaya, Bora Uçar, Kamer Kaya, Ümit V. Çatalyürek. Multilevel Algorithms for Acyclic Partitioning of Directed Acyclic Graphs. *SIAM Journal on Scientific Computing*, 2019, 41 (4), pp.A2117-A2145. 10.1137/18M1176865 . hal-02306566

**HAL Id: hal-02306566**

**<https://inria.hal.science/hal-02306566>**

Submitted on 11 Oct 2019

**HAL** is a multi-disciplinary open access archive for the deposit and dissemination of scientific research documents, whether they are published or not. The documents may come from teaching and research institutions in France or abroad, or from public or private research centers.

L'archive ouverte pluridisciplinaire **HAL**, est destinée au dépôt et à la diffusion de documents scientifiques de niveau recherche, publiés ou non, émanant des établissements d'enseignement et de recherche français ou étrangers, des laboratoires publics ou privés.

1 **MULTILEVEL ALGORITHMS FOR ACYCLIC PARTITIONING OF**  
2 **DIRECTED ACYCLIC GRAPHS\***

3 JULIEN HERRMANN<sup>†</sup>, M. YUSUF ÖZKAYA<sup>†</sup>, BORA UÇAR<sup>‡</sup>,  
4 KAMER KAYA<sup>§</sup>, AND ÜMIT V. ÇATALYÜREK<sup>†</sup>

5 **Abstract.** We investigate the problem of partitioning the vertices of a directed acyclic graph  
6 into a given number of parts. The objective function is to minimize the number or the total weight  
7 of the edges having end points in different parts, which is also known as edge cut. The standard load  
8 balancing constraint of having an equitable partition of the vertices among the parts should be met.  
9 Furthermore, the partition is required to be *acyclic*, i.e., the inter-part edges between the vertices  
10 from different parts should preserve an acyclic dependency structure among the parts. In this work,  
11 we adopt the multilevel approach with coarsening, initial partitioning, and refinement phases for  
12 acyclic partitioning of directed acyclic graphs. We focus on two-way partitioning (sometimes called  
13 bisection), as this scheme can be used in a recursive way for multi-way partitioning. To ensure  
14 the acyclicity of the partition at all times, we propose novel and efficient coarsening and refinement  
15 heuristics. The quality of the computed acyclic partitions is assessed by computing the edge cut.  
16 We also propose effective ways to use the standard undirected graph partitioning methods in our  
17 multilevel scheme. We perform a large set of experiments on a dataset consisting of (i) graphs  
18 coming from an application and (ii) some others corresponding to matrices from a public collection.  
19 We report significant improvements compared to the current state of the art.

20 **Key words.** directed graph, acyclic partitioning, multilevel partitioning

21 **AMS subject classifications.** 05C70, 05C85, 68R10, 68W05

22 **1. Introduction.** The standard graph partitioning (GP) problem asks for a  
23 partition of the vertices of an undirected graph into a number of parts. The objective  
24 and the constraint of this well-known problem are to minimize the number of edges  
25 having vertices in two different parts and to equitably partition the vertices among  
26 the parts. The GP problem is NP-complete [13, ND14]. We investigate a variant of  
27 this problem, called *acyclic partitioning*, for directed acyclic graphs. In this variant,  
28 we have one more constraint: the partition should be acyclic. In other words, for a  
29 suitable numbering of the parts, all edges should be directed from a vertex in a part  
30  $p$  to another vertex in a part  $q$  where  $p \leq q$ .

31 The directed acyclic graph partitioning (DAGP) problem arises in many appli-  
32 cations. The stated variant of the DAGP problem arises in exposing parallelism in  
33 automatic differentiation [6, Ch.9], and particularly in the computation of the Newton  
34 step for solving nonlinear systems [4, 5]. The DAGP problem with some additional  
35 constraints is used to reason about the parallel data movement complexity and to dy-  
36 namically analyze the data locality potential [10, 11]. Other important applications  
37 of the DAGP problem include (i) fusing loops for improving temporal locality, and en-  
38 abling streaming and array contractions in runtime systems [19], such as Bohrium [20];  
39 (ii) analysis of cache efficient execution of streaming applications on uniprocessors [1];  
40 (iii) a number of circuit design applications in which the signal directions impose  
41 acyclic partitioning requirement [7, 29].

42 Let us consider a toy example shown in Figure 1.1(a). A partition of the vertices

---

\*A preliminary version appeared in CCGRID'17 [15].

<sup>†</sup>School of Computational Science and Engineering, Georgia Institute of Technology, Atlanta, Georgia 30332-0250, [julien.herrmann@cc.gatech.edu](mailto:julien.herrmann@cc.gatech.edu), [myozka@gatech.edu](mailto:myozka@gatech.edu), [umit@gatech.edu](mailto:umit@gatech.edu).

<sup>‡</sup>CNRS and LIP (UMR5668 Université de Lyon - CNRS - ENS Lyon - Inria - UCBL 1), 46, allée d'Italie, ENS Lyon, 69364, France, [bora.ucar@ens-lyon.fr](mailto:bora.ucar@ens-lyon.fr).

<sup>§</sup>Sabancı University, Istanbul, Turkey, [kaya@sabanciuniv.edu](mailto:kaya@sabanciuniv.edu).

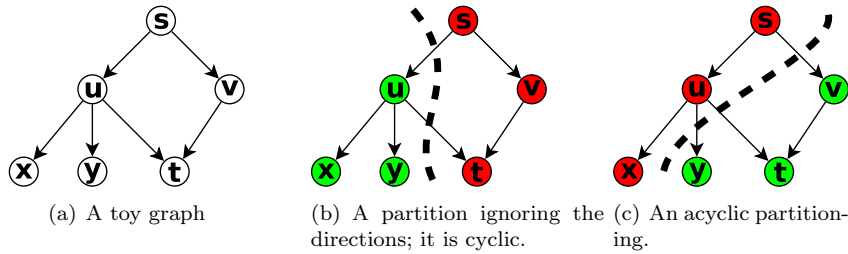


Fig. 1.1: **a)** A toy example with six tasks and six dependencies, **b)** a non-acyclic partitioning when edges are oriented, **c)** an acyclic partitioning of the same directed graph.

43 of this graph is shown in [Figure 1.1\(b\)](#) with a dashed curve. Since there is a cut edge  
 44 from  $s$  to  $u$  and another from  $u$  to  $t$ , the partition is cyclic, and is not acceptable. An  
 45 acyclic partition is shown in [Figure 1.1\(c\)](#), where all the cut edges are from one part  
 46 to the other.

47 We adopt the multilevel partitioning approach [2, 14] with the coarsening, initial  
 48 partitioning, and refinement phases for acyclic partitioning of DAGs. We propose  
 49 heuristics for these three phases ([Subsections 4.1, 4.2 and 4.3](#), respectively) which  
 50 guarantee acyclicity of the partitions at all phases and maintain a DAG at every  
 51 level. We strived to have fast heuristics at the core. With these characterizations,  
 52 the coarsening phase requires new algorithmic/theoretical reasoning, while the initial  
 53 partitioning and refinement heuristics are direct adaptations of the standard methods  
 54 used in undirected graph partitioning, with some differences worth mentioning. We  
 55 discuss only the bisection case, as we were able to improve the direct  $k$ -way algorithms  
 56 we proposed before [15] by using the bisection heuristics recursively—we give a brief  
 57 comparison in [Subsection 5.4](#).

58 The acyclicity constraint on the partitions precludes the use of the state of the  
 59 art undirected graph partitioning tools. This has been recognized before, and those  
 60 tools were put aside [15, 21]. While this is sensible, one can still try to make use of the  
 61 existing undirected graph partitioning tools [14, 16, 25, 27], as they have been very  
 62 well engineered. Let us assume that we have partitioned a DAG with an undirected  
 63 graph partitioning tool into two parts by ignoring the directions. It is easy to detect  
 64 if the partition is cyclic since all the edges need to go from part one to part two.  
 65 Furthermore, we can easily fix it as follows. Let  $v$  be a vertex in the second part;  
 66 we can move all  $u$  vertices for which there is a path from  $v$  to  $u$  into the second  
 67 part. This procedure breaks any cycle containing  $v$  and hence, the partition becomes  
 68 acyclic. However, the edge cut may increase, and the partitions can be unbalanced.  
 69 To solve the balance problem and reduce the cut, we can apply a restricted version  
 70 of the move-based refinement algorithms in the literature. After this step, this final  
 71 partition meets the acyclicity and balance conditions. Depending on the structure  
 72 of the input graph, it could also be a good initial partition for reducing the edge  
 73 cut. Indeed, one of our most effective schemes uses an undirected graph partitioning  
 74 algorithm to create a (potentially cyclic) partition, fixes the cycles in the partition,  
 75 and refines the resulting acyclic partition with a novel heuristic to obtain an initial  
 76 partition. We then integrate this partition within the proposed coarsening approaches  
 77 to refine it at different granularities. We elaborate on this scheme in [Subsection 4.4](#).

78 The rest of the paper is organized as follows: [Section 2](#) introduces the notation

79 and background on directed acyclic graph partitioning and Section 3 briefly surveys  
 80 the existing literature. We propose multilevel partitioning heuristics for acyclic par-  
 81 titioning of directed acyclic graphs in Section 4. Section 5 presents the experimental  
 82 results, and Section 6 concludes the paper.

83 **2. Preliminaries and notation.** A directed graph  $G = (V, E)$  contains a set of  
 84 vertices  $V$  and a set of directed edges  $E$  of the form  $e = (u, v)$ , where  $e$  is directed  
 85 from  $u$  to  $v$ . A path is a sequence of edges  $(u_1, v_1) \cdot (u_2, v_2), \dots$  with  $v_i = u_{i+1}$ . A path  
 86  $((u_1, v_1) \cdot (u_2, v_2) \cdot (u_3, v_3) \cdots (u_\ell, v_\ell))$  is of length  $\ell$ , where it connects a sequence of  
 87  $\ell + 1$  vertices  $(u_1, v_1 = u_2, \dots, v_{\ell-1} = u_\ell, v_\ell)$ . A path is called *simple* if the connected  
 88 vertices are distinct. Let  $u \rightsquigarrow v$  denote a simple path that starts from  $u$  and ends at  
 89  $v$ . A path  $((u_1, v_1) \cdot (u_2, v_2) \cdots (u_\ell, v_\ell))$  forms a (simple) *cycle* if all  $v_i$  for  $1 \leq i \leq \ell$   
 90 are distinct and  $u_1 = v_\ell$ . A *directed acyclic graph*, DAG in short, is a directed graph  
 91 with no cycles.

92 The path  $u \rightsquigarrow v$  represents a dependency of  $v$  to  $u$ . We say that the edge  $(u, v)$   
 93 is *redundant* if there exists another  $u \rightsquigarrow v$  path in the graph. That is, when we  
 94 remove a redundant  $(u, v)$  edge,  $u$  remains to be connected to  $v$ , and hence, the  
 95 dependency information is preserved. We use  $\text{Pred}[v] = \{u \mid (u, v) \in E\}$  to represent  
 96 the (immediate) predecessors of a vertex  $v$ , and  $\text{Succ}[v] = \{u \mid (v, u) \in E\}$  to represent  
 97 the (immediate) successors of  $v$ . We call the neighbors of a vertex  $v$ , its immediate  
 98 predecessors and immediate successors:  $\text{Neigh}[u] = \text{Pred}[v] \cup \text{Succ}[v]$ . For a vertex  $u$ ,  
 99 the set of vertices  $v$  such that  $u \rightsquigarrow v$  are called the *descendants* of  $u$ . Similarly, the  
 100 set of vertices  $v$  such that  $v \rightsquigarrow u$  are called the *ancestors* of the vertex  $u$ . We will  
 101 call vertices without any predecessors (and hence ancestors) as the *sources* of  $G$ , and  
 102 vertices without any successors (and hence descendants) as the *targets* of  $G$ . Every  
 103 vertex  $u$  has a weight denoted by  $w_u$  and every edge  $(u, v) \in E$  has a cost denoted by  
 104  $c_{u,v}$ .

105 A  $k$ -way partitioning of a graph  $G = (V, E)$  divides  $V$  into  $k$  disjoint subsets  
 106  $\{V_1, \dots, V_k\}$ . The weight of a part  $V_i$  denoted by  $w(V_i)$  is equal to  $\sum_{u \in V_i} w_u$ , which  
 107 is the total vertex weight in  $V_i$ . Given a partition, an edge is called a *cut edge* if its  
 108 endpoints are in different parts. The *edge cut* of a partition is defined as the sum of  
 109 the costs of the cut edges. Usually, a constraint on the part weights accompanies the  
 110 problem. We are interested in acyclic partitions, which are defined below.

111 **DEFINITION 2.1 (Acyclic  $k$ -way partition).** A partition  $\{V_1, \dots, V_k\}$  of  $G =$   
 112  $(V, E)$  is called an acyclic  $k$ -way partition if two paths  $u \rightsquigarrow v$  and  $v' \rightsquigarrow u'$  do not  
 113 co-exist for  $u, u' \in V_i$ ,  $v, v' \in V_j$ , and  $1 \leq i \neq j \leq k$ .

114 There is a related definition in the literature [11], which is called a convex par-  
 115 tition. A partition is convex if for all vertex pairs  $u, v$  in the same part, the vertices  
 116 in any  $u \rightsquigarrow v$  path are also in the same part. Hence, if a partition is acyclic it is also  
 117 convex. On the other hand, convexity does not imply acyclicity. Figure 2.1 shows  
 118 that the definitions of an acyclic partition and a convex partition are not equivalent.  
 119 For the toy graph in Figure 2.1(a), there are three possible balanced partitions shown  
 120 in Figure 2.1(b), Figure 2.1(c), and Figure 2.1(d). They are all convex, but only the  
 121 one in Figure 2.1(d) is acyclic.

122 Deciding on the existence of a  $k$ -way acyclic partition respecting an upper bound  
 123 on the part weights and an upper bound on the cost of cut edges is NP-complete [13].  
 124 The formal problem treated in this paper is defined as follows.

125 **DEFINITION 2.2 (DAG partitioning problem).** Given a DAG  $G = (V, E)$  an im-  
 126 balance parameter  $\varepsilon$ , find an acyclic  $k$ -way partition  $P = \{V_1, \dots, V_k\}$  of  $V$  such that

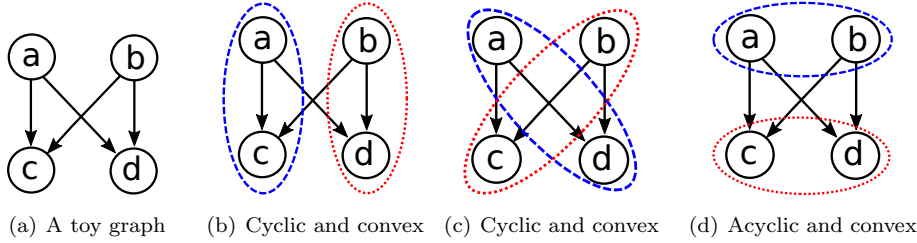


Fig. 2.1: A toy graph (left), two cyclic and convex partitions (middle two), and an acyclic and convex partition (right).

127 *the balance constraints*

$$128 \quad (2.1) \quad w(V_i) \leq (1 + \varepsilon) \frac{\sum_{v \in V} w_v}{k}$$

129 *are satisfied for  $1 \leq i \leq k$ , and the edge cut is minimized.*

130 **3. Related work.** Fauzia et al. [11] propose a heuristic for the acyclic partitioning  
 131 problem to optimize data locality when analyzing DAGs. To create partitions,  
 132 the heuristic categorizes a vertex as ready to be assigned to a partition when all of  
 133 the vertices it depends on have already been assigned. Vertices are assigned to the  
 134 current partition set until the maximum number of vertices that would be “active”  
 135 during the computation of the part reaches a specified limit, which is the cache size  
 136 in their application. This implies that part sizes are not limited by the sum of the  
 137 total vertex weights but is a complex function that depends on an external schedule  
 138 (order) of the vertices. This differs from our problem as we limit the size of each part  
 139 by the total sum of the weights of the vertices on that part.

140 Kernighan [17] proposes an algorithm to find a minimum edge-cut partition of  
 141 the vertices of a graph into subsets of size greater than a lower bound and inferior  
 142 to an upper bound. The partition needs to use a fixed vertex sequence that cannot  
 143 be changed. Indeed, Kernighan’s algorithm takes a topological order of the vertices  
 144 of the graph as an input and partitions the vertices such that all vertices in a subset  
 145 constitute a continuous block in the given topological order. This procedure is optimal  
 146 for a given, fixed topological order and has a run time proportional to the number  
 147 of edges in the graph, if the part weights are taken as constant. We used a modified  
 148 version of this algorithm as a heuristic in the earlier version of our work [15].

149 Cong et al. [7] describe two approaches for obtaining acyclic partitions of di-  
 150 rected Boolean networks, modeling circuits. The first one is a single-level Fiduccia-  
 151 Mattheyses (FM)-based approach. In this approach, Cong et al. generate an initial  
 152 acyclic partition by splitting the list of the vertices (in a topological order) from left  
 153 to right into  $k$  parts such that the weight of each part does not violate the bound.  
 154 The quality of the results is then improved with a  $k$ -way variant of the FM heuristic  
 155 [12] taking the acyclicity constraint into account. Our previous work [15] employs  
 156 a similar refinement heuristic. The second approach of Cong et al. is a two-level  
 157 heuristic; the initial graph is first clustered with a special decomposition, and then it  
 158 is partitioned using the first heuristic.

159 In a recent paper [21], Moreira et al. focus on an imaging and computer vision  
 160 application on embedded systems and discuss acyclic partitioning heuristics. They

161 propose a single level approach in which an initial acyclic partitioning is obtained  
 162 using a topological order. To refine the partitioning, they proposed four local search  
 163 heuristics which respect the balance constraint and maintain the acyclicity of the  
 164 partition. Three heuristics pick a vertex and move it to an eligible part if and only if  
 165 the move improves the cut. These three heuristics differ in choosing the set of eligible  
 166 parts for each vertex; some are very restrictive, and some allow arbitrary target parts  
 167 as long as acyclicity is maintained. The fourth heuristic tentatively realizes the moves  
 168 that increase the cut in order to escape from a possible local minima. It has been  
 169 reported that this heuristic delivers better results than the others. In a follow-up  
 170 paper, Moreira et al. [22] discuss a multilevel graph partitioner and an evolutionary  
 171 algorithm based on this multilevel scheme. Their multilevel scheme starts with a  
 172 given acyclic partition. Then, the coarsening phase contracts edges that are in the  
 173 same part until there is no edge to contract. Here, matching-based heuristics from  
 174 undirected graph partitioning tools are used without taking the directions of the  
 175 edges into account. Therefore, the coarsening phase can create cycles in the graph;  
 176 however the induced partitions are never cyclic. Then, an initial partition is obtained,  
 177 which is refined during the uncoarsening phase with move-based heuristics. In order  
 178 to guarantee acyclic partitions, the vertices that lie in cycles are not moved. In a  
 179 systematic evaluation of the proposed methods, Moreira et al. note that there are  
 180 many local minima and suggest using relaxed constraints in the multilevel setting.  
 181 The proposed methods have high run time, as the evolutionary method of Moreira  
 182 et al. is not concerned with this issue. Improvements with respect to the earlier  
 183 work [21] are reported.

184 Previously, we had developed a multilevel partitioner [15]. In this paper, we  
 185 propose methods to use an undirected graph partitioner to guide the multilevel par-  
 186 titioner. We focus on partitioning the graph in two parts since we can handle the  
 187 general case with a recursive bisection scheme. We also propose new coarsening, ini-  
 188 tial partitioning, and refinement methods specifically designed for the 2-partitioning  
 189 problem. Our multilevel scheme maintains acyclic partitions and graphs through all  
 190 the levels.

191 Other related work on acyclic partitioning of directed graphs include an exact,  
 192 branch-and-bound algorithm by Nossack and Pesch [23] which works on the integer  
 193 programming formulation of the acyclic partitioning problem. This solution is, of  
 194 course, too costly to be used in practice. Wong et al. [29] present a modification of  
 195 the decomposition of Cong et al. [7] for clustering, and use this in a two-level scheme.

196 **4. Directed multilevel graph partitioning.** We propose a new multilevel tool  
 197 for obtaining acyclic partitions of directed acyclic graphs. Multilevel schemes [2, 14]  
 198 form the de-facto standard for solving graph and hypergraph partitioning problems  
 199 efficiently, and used by almost all current state-of-the-art partitioning tools [3, 14, 16,  
 200 25, 27]. Similar to other multilevel schemes, our tool has three phases: the coarsening  
 201 phase, which reduces the number of vertices by clustering them; the initial partitioning  
 202 phase, which finds a partition of the coarsest graph; and the uncoarsening phase, in  
 203 which the initial partition is projected to the finer graphs and refined along the way,  
 204 until a solution for the original graph is obtained.

205 **4.1. Coarsening.** In this phase, we obtain smaller DAGs by coalescing the ver-  
 206 tices, level by level. This phase continues until the number of vertices becomes smaller  
 207 than a specified bound or the reduction on the number of vertices from one level to the  
 208 next one is lower than a threshold. At each level  $\ell$ , we start with a finer acyclic graph  
 209  $G_\ell$ , compute a valid clustering  $\mathcal{C}_\ell$  ensuring the acyclicity, and obtain a coarser acyclic



210 graph  $G_{\ell+1}$ . While our previous work [15] discussed matching based algorithms for  
 211 coarsening, we present agglomerative clustering based variants here. The new vari-  
 212 ants supersede the matching based ones. Unlike the standard undirected graph case,  
 213 in DAG partitioning, not all vertices can be safely combined. Consider a DAG with  
 214 three vertices  $a, b, c$  and three edges  $(a, b), (b, c), (a, c)$ . Here, the vertices  $a$  and  $c$   
 215 cannot be combined, since that would create a cycle. We say that a set of vertices is  
 216 contractible (all its vertices are matchable), if unifying them does not create a cycle.  
 217 We now present a general theory about finding clusters without forming cycles, after  
 218 giving some definitions.

219 **DEFINITION 4.1 (Clustering).** *A clustering of a DAG is a set of disjoint subsets*  
 220 *of vertices. Note that we do not make any assumptions on whether the subsets are*  
 221 *connected or not.*

222 **DEFINITION 4.2 (Coarse graph).** *Given a DAG  $G$  and a clustering  $C$  of  $G$ , we*  
 223 *let  $G_{|C}$  denote the coarse graph created by contracting all sets of vertices of  $C$ .*

224 The vertices of the coarse graph are the clusters in  $C$ . If  $(u, v) \in G$  for two  
 225 vertices  $u$  and  $v$  that are located in different clusters of  $C$  then  $G_{|C}$  has an (directed)  
 226 edge from the vertex corresponding to  $u$ 's cluster, to the vertex corresponding to  $v$ 's  
 227 cluster.

228 **DEFINITION 4.3 (Feasible clustering).** *A feasible clustering  $C$  of a DAG  $G$  is*  
 229 *a clustering such that  $G_{|C}$  is acyclic.*

230 **THEOREM 4.1.** *Let  $G = (V, E)$  be a DAG. For  $u, v \in V$  and  $(u, v) \in E$ , the coarse*  
 231 *graph  $G_{|\{(u,v)\}}$  is acyclic if and only if there is no path from  $u$  to  $v$  in  $G$  avoiding the*  
 232 *edge  $(u, v)$ .*

233 *Proof.* Let  $G' = (V', E') = G_{|\{(u,v)\}}$  be the coarse graph, and  $w$  be the merged,  
 234 coarser vertex of  $G'$  corresponding to  $\{u, v\}$ .

235 If there is a path from  $u$  to  $v$  in  $G$  avoiding the edge  $(u, v)$ , then all the edges of  
 236 this path are also in  $G'$ , and the corresponding path in  $G'$  goes from  $w$  to  $w$ , creating  
 237 a cycle.

238 Assume that there is a cycle in the coarse graph  $G'$ . This cycle has to pass through  
 239  $w$ ; otherwise, it must be in  $G$  which is impossible by the definition of  $G$ . Thus, there  
 240 is a cycle from  $w$  to  $w$  in the coarse graph  $G'$ . Let  $a \in V'$  be the first vertex visited  
 241 by this cycle after  $w$  and  $b \in V'$  be the last one, just before completing the cycle. Let  
 242  $\mathbf{p}$  be an  $a \rightsquigarrow b$  path in  $G'$  such that  $(w, a) \cdot \mathbf{p} \cdot (b, w)$  is the said  $w \rightsquigarrow w$  cycle in  $G'$ .  
 243 Note that  $a$  can be equal to  $b$  and in this case  $\mathbf{p} = \emptyset$ . By the definition of the coarse  
 244 graph  $G'$ ,  $a, b \in V$  and all edges in the path  $\mathbf{p}$  are in  $E \setminus \{(u, v)\}$ . Since we have a  
 245 cycle in  $G'$ , the following two items must hold:

- 246 • (i) either  $(u, a) \in E$  or  $(v, a) \in E$ , or both; and
- 247 • (ii) either  $(b, u) \in E$  or  $(b, v) \in E$ , or both.

248 Hence, overall we have nine ( $3 \times 3$ ) cases. Here, we investigate only four of them, as the  
 249 “both” conditions in (i) and (ii) can be eliminated easily by the following statements.

- 250 •  $(u, a) \in E$  and  $(b, u) \in E$  is impossible because otherwise,  $(u, a) \cdot \mathbf{p} \cdot (b, u)$   
 251 would be a  $u \rightsquigarrow u$  cycle in the original graph  $G$ .
- 252 •  $(v, a) \in E$  and  $(b, v) \in E$  is impossible because otherwise,  $(v, a) \cdot \mathbf{p} \cdot (b, v)$   
 253 would be a  $v \rightsquigarrow v$  cycle in the original graph  $G$ .
- 254 •  $(v, a) \in E$  and  $(b, u) \in E$  is impossible because otherwise,  $(u, v) \cdot (v, a) \cdot \mathbf{p} \cdot (b, u)$   
 255 would be a  $u \rightsquigarrow u$  cycle in the original graph  $G$ .

256 Thus  $(u, a) \in E$  and  $(b, v) \in E$ . Therefore,  $(u, a) \cdot \mathbf{p} \cdot (b, v)$  is a  $u \rightsquigarrow v$  path in  $G$   
 257 avoiding the edge  $(u, v)$ , which concludes the proof.  $\square$

258 **Theorem 4.1** can be extended to a set of vertices by noting that this time all  
 259 paths connecting two vertices of the set should contain only the vertices of the set.  
 260 The theorem (nor its extension) does not imply an efficient algorithm, as it requires  
 261 at least one transitive reduction. Furthermore, it does not describe a condition about  
 262 two clusters forming a cycle, even if both are individually contractible. In order to  
 263 address both of these issues, we put a constraint on the vertices that can form a  
 264 cluster, based on the following definition.

265 **DEFINITION 4.4 (Top level value).** *For a DAG  $G = (V, E)$ , the top level value*  
 266 *of a vertex  $u \in V$  is the length of the longest path from a source of  $G$  to that vertex.*  
 267 *The top level values of all vertices can be computed in a single traversal of the graph*  
 268 *with a complexity  $O(|V| + |E|)$ . We use  $\text{top}[u]$  to denote the top level of the vertex  $u$ .*

269 The top level value of a vertex is independent of the topological order used for  
 270 computation. By restricting the set of edges considered in the clustering to the edges  
 271  $(u, v) \in E$  such that  $\text{top}[u] + 1 = \text{top}[v]$ , we ensure that no cycles are formed by  
 272 contracting a unique cluster (the condition identified in **Theorem 4.1** is satisfied). Let  
 273  $C$  be a clustering of the vertices. Every edge in a cluster of  $C$  being contractible is a  
 274 necessary condition for  $C$  to be feasible, but not a sufficient one. More restrictions on  
 275 the edges of vertices inside the clusters should be found to ensure that  $C$  is feasible.  
 276 We propose three coarsening heuristics based on clustering sets of more than two  
 277 vertices, whose pair-wise top level differences are always zero or one.

278 **4.1.1. Acyclic clustering with forbidden edges.** To have an efficient heuris-  
 279 tic, we rely only on static information computable in linear time while searching for  
 280 a feasible clustering. As stated in the introduction of this section, we rely on the  
 281 top level difference of one (or less) for all vertices in the same cluster, and an addi-  
 282 tional condition to ensure that there will be no cycles when a number of clusters are  
 283 contracted simultaneously. In **Theorem 4.2**, we give two sufficient conditions for a  
 284 clustering to be feasible (that is, the graphs at all levels are DAGs) and prove their  
 285 correctness.

286 **THEOREM 4.2 (Correctness of the proposed clustering).** *Let  $G = (V, E)$  be a*  
 287 *DAG and  $C = \{C_1, \dots, C_k\}$  be a clustering. If  $C$  is such that:*

- 288 • *for any cluster  $C_i$ , for all  $u, v \in C_i$ ,  $|\text{top}[u] - \text{top}[v]| \leq 1$ ,*
- 289 • *for two different clusters  $C_i$  and  $C_j$  and for all  $u \in C_i$  and  $v \in C_j$  either*  
 290  *$(u, v) \notin E$ , or  $\text{top}[u] \neq \text{top}[v] - 1$ ,*

291 *then, the coarse graph  $G|_C$  is acyclic.*

292 *Proof.* Let us assume (for the sake of contradiction) that there is a clustering  
 293 with the same properties above, but the coarsened graph has a cycle. We pick one  
 294 such clustering  $C = \{C_1, \dots, C_k\}$  with the minimum number of clusters. Let  $t_i =$   
 295  $\min\{\text{top}[u], u \in C_i\}$  be the smallest top level value of a vertex of  $C_i$ . According to the  
 296 properties of  $C$ , for every vertex  $u \in C_i$ , either  $\text{top}[u] = t_i$ , or  $\text{top}[u] = t_i + 1$ . Let  $w_i$   
 297 be the coarse vertex in  $G|_C$  obtained by contracting all vertices in  $C_i$ , for  $i = 1, \dots, k$ .  
 298 By the assumption, there is a cycle in  $G|_C$ , and let  $\mathbf{c}$  be one with the minimum length.  
 299 This cycle passes through all the  $w_i$  vertices. Otherwise, there would be a smaller  
 300 cardinality clustering with the properties above and creating a cycle in the coarsened  
 301 graph, contradicting the minimal cardinality of  $C$ . Let us renumber, without loss of  
 302 generality, the  $w_i$  vertices such that  $\mathbf{c}$  is a  $w_1 \rightsquigarrow w_1$  cycle which passes through all  
 303 the  $w_i$  vertices in the non-decreasing order of the indices. This also renumbers the  
 304 clusters accordingly.

305 After renumbering the  $w_i$  vertices, for every  $i \in \{1, \dots, k\}$ , there is a path in  $G|_C$



306 from  $w_i$  to  $w_{i+1}$ . Given the definition of the coarsened graph, for every  $i \in \{1, \dots, k\}$   
 307 there exists a vertex  $u_i \in C_i$ , and a vertex  $u_{i+1} \in C_{i+1}$  such that there exists a  
 308 path  $u_i \rightsquigarrow u_{i+1}$  in  $G$ . Thus,  $\text{top}[u_i] + 1 \leq \text{top}[u_{i+1}]$ . According to the second  
 309 property, either there is at least one intermediate vertex between  $u_i$  and  $u_{i+1}$  and  
 310 then  $\text{top}[u_i] + 1 < \text{top}[u_{i+1}]$ ; or  $\text{top}[u_i] + 1 \neq \text{top}[u_{i+1}]$  and then  $\text{top}[u_i] + 1 <$   
 311  $\text{top}[u_{i+1}]$ . Thus, in any case,  $\text{top}[u_i] + 1 < \text{top}[u_{i+1}]$  which can be rewritten as  
 312  $\text{top}[u_i] < \text{top}[u_{i+1}] - 1$ .

313 By definition, we know that  $t_i \leq \text{top}[u_i]$  and  $\text{top}[u_{i+1}] - 1 \leq t_{i+1}$ . Thus for every  
 314  $i \in \{1, \dots, k\}$ , we have  $t_i < t_{i+1}$ , which leads to the self-contradicting statement  
 315  $t_1 < t_{k+1} = t_1$  and concludes the proof.  $\square$

316 The main heuristic based on [Theorem 4.2](#) is described in [Algorithm 1](#). This  
 317 heuristic visits all vertices in an order, and adds the visited vertex to a cluster, if  
 318 certain criteria are met; if not, the vertex stays as a singleton. When visiting a  
 319 singleton vertex, the clusters of its in-neighbors and out-neighbors are investigated,  
 320 and the best (according to an objective value) among those meeting the criterion  
 321 described in [Theorem 4.2](#) is selected.

322 [Algorithm 1](#) returns the `leader` array of each vertex for the current coarsening  
 323 step. Vertices with the same leader form a cluster (and will form a single vertex in  
 324 the coarsened graph). For each vertex  $u \in V$ , `leader[u]` is the id of the representative  
 325 vertex for the cluster that will contain  $u$  after [Algorithm 1](#). The `leader` table will  
 326 be used to build the coarse graph. Any arbitrary vertex in a given cluster can be  
 327 used as the leader of this cluster without impacting the rest of the algorithm. At the  
 328 beginning, each vertex belongs to a singleton cluster, and `leader[u] = u`. To keep  
 329 the track of trivial clusters (singleton vertices), we use an auxiliary `mark` array. The  
 330 value `mark[u]` is *false* if  $u$  still belongs to a singleton cluster. Otherwise, the value is  
 331 set to *true*.

332 For each singleton vertex  $u$ , we maintain an auxiliary array `nbbadneighbors` to  
 333 keep the number of non-trivial *bad neighbor* clusters. That is to say, the number  
 334 of clusters containing a neighbor of  $u$  that would violate the second condition of  
 335 [Theorem 4.2](#) in case  $u$  was put in another cluster. Hence, if  $u$  has only one *bad*  
 336 *neighbor* cluster, it can only be put into this cluster. For instance in [Figure 4.1\(a\)](#),  
 337 at this point of the coarsening, vertex  $B$  can only be put in Cluster 1. Otherwise, if  
 338 vertex  $B$  was matched with one of its other neighbors, the second condition of the  
 339 theorem would be violated. Thus, if a vertex has more than one *bad neighbor* in  
 340 different clusters, it has to stay as a singleton. For instance in [Figure 4.1\(b\)](#), vertex  
 341  $B$  has two bad neighbor clusters and cannot be put in any cluster without violating  
 342 the second condition of [Theorem 4.2](#). To check if there exists another bad neighbor  
 343 cluster previously formed, we maintain an array `leaderbadneighbor` that keeps the  
 344 representative/leader of the first bad neighbor cluster for each vertex. Initially, this  
 345 value is set to minus one.

346 In [Algorithm 1](#), the function `ValidNeighbors` selects the *compatible neighbors* of  
 347 vertex  $u$ , that is the neighbors in clusters that vertex  $u$  can join. This selection is  
 348 based on the top level difference (to respect the first condition of [Theorem 4.2](#)), the  
 349 number of *bad neighbors* of  $u$ , and  $u$ 's neighbors (to respect the second condition of  
 350 [Theorem 4.2](#)), and the size limitation (we do not want a cluster to be bigger than  
 351 10% of the total weight of the graph). Then, a best neighbor, `BestNeigh`, according  
 352 to an objective value, such as the edge cost, is selected. After setting the leader of  
 353 vertex  $u$  to the same value as the leader of `BestNeigh`, some bookkeeping is done  
 354 for the arrays related to the second condition of [Theorem 4.2](#). More precisely, at

355 Lines 16–22 of Algorithm 1, the neighbors of  $u$  are informed about  $u$  joining a new  
 356 cluster, potentially becoming a bad neighbor. While doing that, the algorithm skips  
 357 the vertices  $v$  such that  $|\text{top}[u] - \text{top}[v]| > 1$ , since  $u$  cannot form a bad neighbor  
 358 cluster for such  $v$ . Similarly, if the best neighbor chosen for  $u$  was not in a cluster  
 359 previously, i.e., was a singleton vertex, the number of *bad neighbors* of its neighbors  
 360 are updated (Lines 24–30).

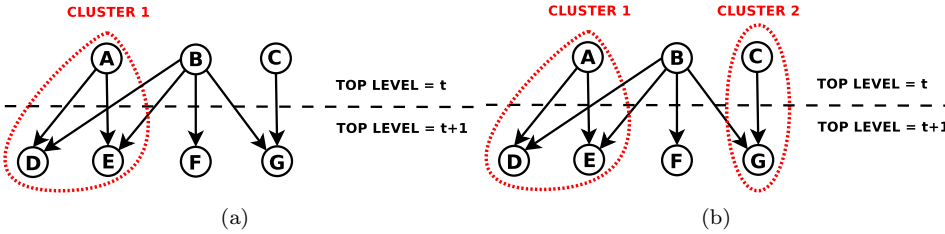


Fig. 4.1: Two examples of acyclic clustering.

361 In our framework, we also implemented the version in the preliminary study [15]  
 362 where the size of cluster is limited to two, meaning that it computes a matching of  
 363 the vertices.

364 It can be easily seen that Algorithm 1 has a worst case time complexity of  $O(|V| +$   
 365  $|E|)$ . The array  $\text{top}$  is constructed in  $O(|V| + |E|)$  time, and the best, valid neighbor  
 366 of a vertex  $u$  is found in  $O(|\text{Neigh}[u]|)$  time. The neighbors of a vertex are visited at  
 367 most once to keep the arrays related to the second condition of Theorem 4.2 up to  
 368 date at Lines 16 and 24.

369 **4.1.2. Acyclic clustering with cycle detection.** We now propose a less re-  
 370 strictive clustering algorithm to ensure that the acyclicity of the coarse graph is  
 371 maintained. As in the previous section, we rely on the top level difference of one  
 372 (or less) for all vertices in the same cluster, i.e., for any cluster  $C_i$ , for all  $u, v \in C_i$ ,  
 373  $|\text{top}[u] - \text{top}[v]| \leq 1$ . Knowing this invariant, when a new vertex is added to a cluster,  
 374 a cycle-detection algorithm checks that no cycles are formed when all the clusters are  
 375 contracted simultaneously. This algorithm does not traverse the entire graph by also  
 376 using the fact that the top level difference within a cluster is at most one.

377 From the proof of Theorem 4.2, we know that with a feasible clustering, if adding  
 378 a vertex to a cluster whose vertices' top level values are  $t$  and  $t + 1$  creates a cycle  
 379 in the contracted graph, then this cycle goes through only the vertices with top level  
 380 values  $t$  or  $t + 1$ . Thus, when considering the addition of a vertex  $u$  to a cluster  $C$   
 381 containing  $v$ , we check potential cycle formations by traversing the graph starting  
 382 from  $u$  in a breadth-first manner in the *DetectCycle* function used in Algorithm 2.  
 383 Let  $t$  denote the minimum top level in  $C$ . When at a vertex  $w$ , we normally add a  
 384 successor  $y$  of  $w$  into the queue, if  $|\text{top}(y) - t| \leq 1$ ; if  $w$  is in the same cluster as one  
 385 of its predecessors  $x$ , we also add  $x$  to the queue if  $|\text{top}(x) - t| \leq 1$ . This function  
 386 uses markers to not to visit the same vertex multiple times, returns *true* if at some  
 387 point in the traversal a vertex from cluster  $C$  is reached, and returns *false*, otherwise.  
 388 In the worst-case, this cycle detection algorithm completes a full graph traversal but  
 389 in practice, it stops quickly and does not introduce a significant overhead.

390 Here, we propose different clustering strategies. These algorithms consider all  
 391 the vertices in the graph, one by one, and put them in a cluster if their top level

**Algorithm 1:** Clustering with forbidden edges

---

```

Data: Directed graph  $G = (V, E)$ , a traversal order of the vertices in  $V$ , a priority on
edges
Result: The leader array for the coarsening
1 top  $\leftarrow$  CompTopLevels( $G$ )
/* Initialize all the auxiliary data to be used */
2 for  $u \in V$  do
3   mark[ $u$ ]  $\leftarrow$  false // all vertices are marked as singleton
4   leader[ $u$ ]  $\leftarrow$   $u$ 
5   weight[ $u$ ]  $\leftarrow$   $w_u$  // keeps the total weight for each cluster
/* nbbadneighbors[ $u$ ] stores the number of bad clusters for a vertex  $u$ . If
it exceeds one,  $u$  is left alone (the second condition of Theorem 4.2.).
*/
6   nbbadneighbors[ $u$ ]  $\leftarrow$  0
7   leaderbadneighbors[ $u$ ]  $\leftarrow$  -1
8 for  $u \in V$  following the traversal order in input do
9   if mark[ $u$ ] then continue
/* The function ValidNeighbors returns the set of valid match candidates
for  $u$  based on Theorem 4.2. It also checks the threshold for the
maximum cluster size, and the number of bad neighbor clusters for  $u$ . */
10   $N \leftarrow$  ValidNeighbors( $u, G, nbbadneighbors, leaderbadneighbors, weight$ )
11  if  $N = \emptyset$  then continue
12  BestNeigh  $\leftarrow$  BestNeighbour( $N$ )
13   $\ell \leftarrow$  leader[BestNeigh]
14  leader[ $u$ ]  $\leftarrow$   $\ell$  // assign  $u$  to BestNeigh's cluster
15  weight[ $\ell$ ]  $\leftarrow$  weight[ $\ell$ ] +  $w_u$ 
/* Let the neighbors of  $u$  know that it is not a singleton anymore */
16  for  $v \in$  Neigh[ $u$ ] do
17    if  $|\text{top}[u] - \text{top}[v]| > 1$  then continue //  $u$  cannot form a bad cluster
18    if nbbadneighbors[ $v$ ] = 0 then
19      nbbadneighbors[ $v$ ]  $\leftarrow$  1
20      leaderbadneighbors[ $v$ ]  $\leftarrow$   $\ell$ 
21    else if nbbadneighbors[ $v$ ] = 1 and leaderbadneighbors[ $v$ ]  $\neq$   $\ell$  then
22      nbbadneighbors[ $v$ ]  $\leftarrow$  2 // mark  $v$  as unmatchable
/* If BestNeigh was forming a singleton cluster before  $u$ 's assignment */
23  if mark[BestNeigh] = false then
/* Let BestNeigh's neighbors know that it is not a singleton anymore */
24    for  $v \in$  Neigh[BestNeigh] do
25      if  $|\text{top}[BestNeigh] - \text{top}[v]| > 1$  then continue
26      if nbbadneighbors[ $v$ ] = 0 then
27        nbbadneighbors[ $v$ ]  $\leftarrow$  1 // The first bad neighbor cluster for  $v$ 
28        leaderbadneighbors[ $v$ ]  $\leftarrow$   $\ell$ 
29      else if nbbadneighbors[ $v$ ] = 1 and leaderbadneighbors[ $v$ ]  $\neq$   $\ell$  then
30        nbbadneighbors[ $v$ ]  $\leftarrow$  2 // mark  $v$  as unmatchable
31    mark[BestNeigh]  $\leftarrow$  true // BestNeigh is not a singleton anymore
32  mark[ $u$ ]  $\leftarrow$  true //  $u$  is not a singleton anymore
33 return leader

```

---

392 differences are at most one and if no cycles are introduced. The clustering algorithms  
393 depending on different vertex traversal orders and priority definitions on the adjacent  
394 edges are described in Algorithm 2. As Algorithm 1, this algorithm also returns the  
395 leader array of each vertex for the current coarsening step. When a vertex is put in a  
396 cluster with top level values  $t$  and  $t + 1$ , its *markup* (respectively *markdown*) value is  
397 set to *true* if its top level value is  $t$  (respectively  $t + 1$ ). Since the worst case complexity  
398 of the cycle detection is  $O(|V| + |E|)$ , the worst case complexity of Algorithm 2 is  
399  $O(|V|(|V| + |E|))$ . However, the cycle detection stops quickly in practice and the

400 behavior of Algorithm 2 is closer to  $O(|V| + |E|)$  as described in Subsection 5.6.

---

**Algorithm 2:** Clustering with cycle detection
 

---

**Data:** Directed graph  $G = (V, E)$ , a traversal order of the vertices in  $V$ , a priority on edges  
**Result:** A feasible clustering  $C$  of  $G$

```

1 top  $\leftarrow$  CompTopLevels( $G$ )
2 for  $u \in V$  do
3   markup[ $u$ ]  $\leftarrow$  false // if  $u$ 's cluster has a  $v$  with  $\text{top}[v] = \text{top}[u] + 1$ 
4   markdown[ $u$ ]  $\leftarrow$  false // if  $u$ 's cluster has a  $v$  with  $\text{top}[v] = \text{top}[u] - 1$ 
5   leader[ $u$ ]  $\leftarrow$   $u$  // the leader vertex id for  $u$ 's cluster
6 for  $u \in V$  following the traversal order in input do
7   if markup[ $u$ ] or markdown[ $u$ ] then continue
8   for  $v \in \text{Neigh}[u]$  following given priority on edges do
9     if  $(|\text{top}[u] - \text{top}[v]| > 1)$  then continue // we use  $|\text{top}[u] - \text{top}[v]| = 1$ 
10    /* If this is a  $(u, v)$  edge */
11    if  $v \in \text{Succ}[u]$  then
12      if markup[ $v$ ] then continue
13      if DetectCycle( $u, v, G, \text{leader}$ ) then continue
14      leader[ $u$ ]  $\leftarrow$  leader[ $v$ ]
15      markup[ $u$ ]  $\leftarrow$  markdown[ $v$ ]  $\leftarrow$  true
16    /* If this is a  $(v, u)$  edge */
17    if  $v \in \text{Pred}[u]$  then
18      if markdown[ $v$ ] then continue
19      if DetectCycle( $u, v, G, \text{leader}$ ) then continue
20      leader[ $u$ ]  $\leftarrow$  leader[ $v$ ]
21      markdown[ $u$ ]  $\leftarrow$  markup[ $v$ ]  $\leftarrow$  true
22 return leader

```

---

401 **4.1.3. Hybrid acyclic clustering.** The cycle detection based algorithm can  
 402 suffer from quadratic run time for vertices with large in-degrees or out-degrees. To  
 403 avoid this, we design a hybrid acyclic clustering which uses the clustering strategy  
 404 described in Algorithm 2 by default and switches to the clustering strategy in Al-  
 405 gorithm 1 for *large degree* vertices. We define a limit on the degree of a vertex  
 406 (typically  $\sqrt{|V|}/10$ ) for calling it *large degree*. When considering an edge  $(u, v)$  where  
 407  $\text{top}[u] + 1 = \text{top}[v]$ , if the degrees of  $u$  and  $v$  do not exceed the limit, we use the cycle  
 408 detection algorithm to determine if we can contract the edge. Otherwise, if the out-  
 409 degree of  $u$  or the indegree of  $v$  is too large, the edge will be contracted if Algorithm 1  
 410 allows so. The complexity of this algorithm is in between those of Algorithm 1 and  
 411 Algorithm 2 and will likely avoid the quadratic behavior in practice (if not, the degree  
 412 parameter can be adapted).

413 **4.2. Initial partitioning.** After the coarsening phase, we compute an initial  
 414 acyclic partitioning of the coarsest graph. We present two heuristics. One of them  
 415 is akin to the greedy graph growing method used in the standard graph/hypergraph  
 416 partitioning methods. The second one uses an undirected partitioning and then fixes  
 417 the acyclicity of the partitions. Throughout this section, we use  $(V_0, V_1)$  to denote  
 418 the bisection of the vertices of the coarsest graph  $G$ . The acyclic bisection  $(V_0, V_1)$  is  
 419 such that there is no edge from the vertices in  $V_1$  to those in  $V_0$ .

420 **4.2.1. Greedy directed graph growing.** One approach to compute a bisection of a directed graph is to design a greedy algorithm that moves vertices from one part to another using local information. Greedy algorithms have shown to be effective for initial partitioning in multilevel schemes in the undirected case. We start with all vertices in  $V_1$  and replace vertices towards  $V_0$  by using heaps. At any time, the vertices that can be moved to  $V_0$  are in the heap. These vertices are those whose all in-neighbors are in  $V_0$ . Initially only the sources are in the heap, and when all the in-neighbors of a vertex  $v$  are moved to the first part,  $v$  is inserted into the heap. We separate this process into two phases. In the first phase, the key-values of the vertices in the heap are set to the weighted sum of their incoming edges, and the ties are broken in favor of the vertex closer to the first vertex moved. The first phase continues until the first part has more than 0.9 of the maximum allowed weight (modulo the maximum weight of a vertex). In the second phase, the actual gain of a vertex is used. This gain is equal to the sum of the weights of the incoming edges minus the sum of the weights of the outgoing edges. In this phase, the ties are broken in favor of the heavier vertices. The second phase stops as soon as the required balance is obtained. The reason that we separated this heuristic into two phases is that at the beginning, the gains are of no importance, and the more vertices become movable the more flexibility the heuristic has. Yet, towards the end, parts are fairly balanced, and using actual gains can help keeping the cut small.

440 Since the order of the parts is important, we also reverse the roles of the parts, and the directions of the edges. That is, we put all vertices in  $V_0$ , and move the vertices one by one to  $V_1$ , when all out-neighbors of a vertex have been moved to  $V_1$ . The proposed greedy directed graph growing heuristic returns the best of the these two alternatives.

445 **4.2.2. Undirected bisection and fixing acyclicity.** In this heuristic, we partition the coarsest graph as if it were undirected and then move the vertices from one part to another in case the partition was not acyclic. Let  $(P_0, P_1)$  denote the (not necessarily acyclic) bisection of the coarsest graph treated as if it were undirected.

449 The proposed approach designates arbitrarily  $P_0$  as  $V_0$  and  $P_1$  as  $V_1$ . One way to fix the cycle is to move all ancestors of the vertices in  $V_0$  to  $V_0$ , thereby guaranteeing that there is no edge from vertices in  $V_1$  to vertices in  $V_0$ , making the bisection  $(V_0, V_1)$  acyclic. We do these moves in a reverse topological order, as shown in Algorithm 3. Another way to fix the acyclicity is to move all descendants of the vertices in  $V_1$  to  $V_1$ , again guaranteeing an acyclic partition. We do these moves in a topological order, as shown in Algorithm 4. We then fix the possible unbalance with a refinement algorithm.

457 Note that we can also initially designate  $P_1$  as  $V_0$  and  $P_0$  as  $V_1$ , and again use Algorithms 3 and 4 to fix a potential cycle in two different ways. We try all four of these choices, and return the best partition (essentially returning the best of the four choices to fix the acyclicity of  $(P_0, P_1)$ ).

461 **4.3. Refinement.** This phase projects the partition obtained for a coarse graph to the next, finer one and refines the partition by vertex moves. As in the standard refinement methods, the proposed heuristic is applied in a number of passes. Within a pass, we repeatedly select the vertex with the maximum move gain among those that can be moved. We tentatively realize this move if the move maintains or improves the balance. Then, the most profitable prefix of vertex moves are realized at the end of the pass. As usual, we allow the vertices move only once in a pass; therefore once a vertex is moved, it is not eligible to move again during the same pass. We use heaps

**Algorithm 3:** fixAcyclicityUp**Data:** Directed graph  $G = (V, E)$  and a bisection  $part$ **Result:** An acyclic bisection of  $G$ 


---

```

1 for  $u \in G$  (in reverse topological order) do
2   if  $part[u] = 0$  then
3     for  $v \in \text{Pred}[u]$  do
4        $part[v] \leftarrow 0$ 
5 return  $part$ 

```

---

**Algorithm 4:** fixAcyclicityDown**Data:** Directed graph  $G = (V, E)$  and a bisection  $part$ **Result:** An acyclic bisection of  $G$ 


---

```

1 for  $u \in G$  (in topological order) do
2   if  $part[u] = 1$  then
3     for  $v \in \text{Succ}[u]$  do
4        $part[v] \leftarrow 1$ 
5 return  $part$ 

```

---

469 with the gain of moves as the key value, where we keep only movable vertices. We  
470 call a vertex *movable*, if moving it to the other part does not create a cyclic partition.  
471 As previously done, we use the notation  $(V_0, V_1)$  to designate the acyclic bisection  
472 with no edge from vertices in  $V_1$  to vertices in  $V_0$ . This means that for a vertex to  
473 move from part  $V_0$  to part  $V_1$ , one of the two conditions should be met (i) either all its  
474 out-neighbors should be in  $V_1$ ; (ii) or the vertex has no out-neighbors at all. Similarly,  
475 for a vertex to move from part  $V_1$  to part  $V_0$ , one of the two conditions should be met  
476 (i) either all its in-neighbors should be in  $V_0$ ; (ii) or the vertex has no in-neighbors  
477 at all. This is in a sense the adaptation of boundary Fiduccia-Mattheyses [12] (FM)  
478 to directed graphs, where the boundary corresponds to the movable vertices. The  
479 notion of movability being more restrictive results in an important simplification with  
480 respect to the undirected case. The gain of moving a vertex  $v$  from  $V_0$  to  $V_1$  is

$$481 \quad (4.1) \quad \sum_{u \in \text{Succ}[v]} w(v, u) - \sum_{u \in \text{Pred}[v]} w(u, v),$$

482 and the negative of this value when moving it from  $V_1$  to  $V_0$ . This means that the gain  
483 of vertices are static: once a vertex is inserted in the heap with the key value (4.1),  
484 it is never updated. A move could render some vertices unmovable; if they were in  
485 the heap, then they should be deleted. Therefore, the heap data structure needs to  
486 support insert, delete, and extract max operations only.

487 We have also implemented a swapping based refinement heuristic akin to the  
488 boundary Kernighan-Lin [18] (KL), and another one moving vertices only from the  
489 maximum loaded part. For graphs with unit weight vertices, we suggest using the  
490 boundary FM, and for others we suggest using one pass of boundary KL followed by  
491 one pass of the boundary FM that moves vertices only from the maximum loaded  
492 part.

493 **4.4. Constraint coarsening and initial partitioning.** There are a number  
494 of highly successful, undirected graph partitioning libraries [16, 25, 27]. They are



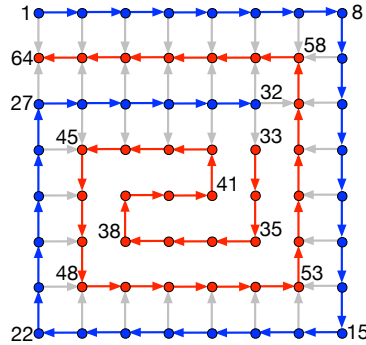


Fig. 4.2:  $8 \times 8$  grid graph whose vertices are ordered in a spiral way; a few of the vertices are labeled with their number. All edges are oriented from a lower numbered vertex to a higher numbered one. There is a unique bipartition with 32 vertices in each side. The edges defining the total order are shown in red and blue, except the one from 32 to 33; the cut edges are shown in gray; other internal edges are not shown.

495 not directly usable for our purposes, as the partitions can be cyclic. Fixing such  
 496 partitions, by moving vertices to break the cyclic dependencies among the parts, can  
 497 increase the edge cut dramatically (with respect to the undirected cut). Consider for  
 498 example, the  $n \times n$  grid graph, where the vertices are integer positions for  $i = 1, \dots, n$   
 499 and  $j = 1, \dots, n$  and a vertex at  $(i, j)$  is connected to  $(i', j')$  when  $|i - i'| = 1$  or  
 500  $|j - j'| = 1$ , but not both. There is an acyclic orientation of this graph, called spiral  
 501 ordering, as described in Figure 4.2 for  $n = 8$ . This spiral ordering defines a total  
 502 order. When the directions of the edges are ignored, we can have a bisection with  
 503 perfect balance by cutting only  $n = 8$  edges with a vertical line. This partition is  
 504 cyclic; and it can be made acyclic by putting all vertices numbered greater than 32  
 505 to the second part. This partition, which puts the vertices 1–32 to the first part and  
 506 the rest to the second part, is the unique acyclic bisection with perfect balance for  
 507 the associated directed acyclic graph. The edge cut in the directed version is 35 as  
 508 seen in the figure (gray edges). In general one has to cut  $n^2 - 4n + 3$  edges for  $n \geq 8$ :  
 509 the blue vertices in the border (excluding the corners) have one edge directed to a red  
 510 vertex; the interior blue vertices have two such edges; finally, the blue vertex labeled  
 511  $n^2/2$  has three such edges.

512 Let us also investigate the quality of the partitions from a more practical stand-  
 513 point. We used MeTiS [16] as the undirected graph partitioner on a dataset of 94  
 514 matrices (their details are in Section 5). The results are given in Figure 4.3. For  
 515 this preliminary experiment, we partitioned the graphs into two with the maximum  
 516 allowed load imbalance  $\varepsilon = 3\%$ . In the experiment, for only two graphs, the output  
 517 of MeTiS is acyclic, and the geometric mean of the normalized edge cut is 0.0012.  
 518 Figure 4.3(a) shows the normalized edge cut and the load imbalance after fixing the  
 519 cycles, while Figure 4.3(b) shows the two measurements after meeting the balance  
 520 criteria. A normalized edge cut value is computed by normalizing the edge cut with  
 521 respect to the number of edges.

522 In both figures, the horizontal lines mark the geometric mean of the normalized  
 523 edge cuts, and the vertical lines mark the 3% imbalance ratio. In Figure 4.3(a), there  
 524 are 37 instances in which the load balance after fixing the cycles is feasible. The

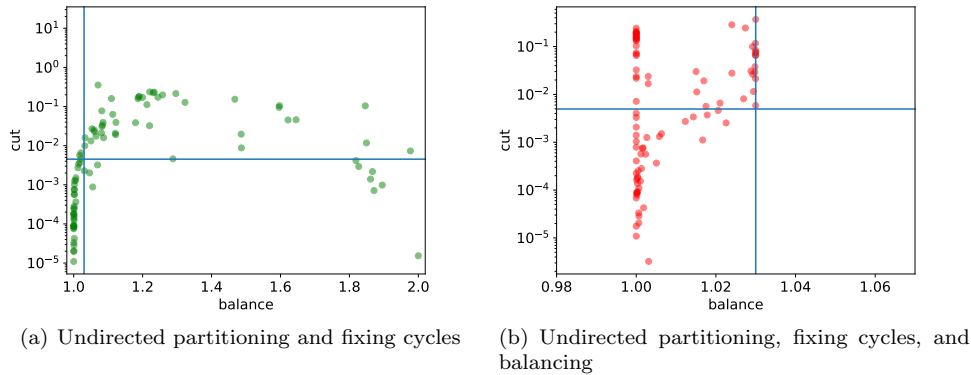


Fig. 4.3: Normalized edge cut (normalized with respect to the number of edges), and the balance obtained after using an undirected graph partitioner and fixing the cycles (left), and after ensuring balance with refinement (right).

525 geometric mean of the normalized edge cuts in this subfigure is 0.0045, while in the  
 526 other subfigure, it is 0.0049. Fixing the cycles increases the edge cut with respect to  
 527 an undirected partitioning, but not catastrophically (only by  $0.0045/0.0012 = 3.75$   
 528 times in these experiments), and achieving balance after this step increases the cut  
 529 only a little (goes to 0.0049 from 0.0045). That is why we suggest using an undirected  
 530 graph partitioner, fixing the cycles among the parts, and performing a refinement  
 531 based method for load balancing as a good (initial) partitioner.

532 In order to refine the initial partition in a multilevel setting, we propose a scheme  
 533 similar to the *iterated multilevel algorithm* used in the existing partitioners [3, 28]. In  
 534 this scheme, first a partition  $P$  is obtained. Then, the coarsening phase is employed  
 535 to match (or to agglomerate) the vertices that were in the same part in  $P$ . After  
 536 the coarsening, an initial partitioning is freely available by using the partition  $P$   
 537 on the coarsest graph. The refinement phase then can work as before. Moreira  
 538 et al. [22] use this approach for the directed graph partitioning problem. To be  
 539 more concrete, we first use an undirected graph partitioner, then fix the cycles as  
 540 discussed in Section 4.2.2, and then refine this acyclic partition for balance with the  
 541 proposed refinement heuristics in Subsection 4.3. We then use this acyclic partition for  
 542 constraint coarsening and initial partitioning. We expect this scheme to be successful  
 543 in graphs with many sources and targets where the sources and targets can lie in any  
 544 of the parts while the overall partition is acyclic. On the other hand, if a graph is such  
 545 that its balanced acyclic partitions need to put sources in one part and the targets in  
 546 another part, then fixing acyclicity may result in moving many vertices. This in turn  
 547 will harm the edge cut found by the undirected graph partitioner.

548 **5. Experimental evaluation.** The partitioning tool presented (`dagP`) is imple-  
 549 mented in C/C++ programming languages. The experiments are conducted on a  
 550 computer equipped with dual 2.1 GHz, Xeon E5-2683 processors and 512GB memory.  
 551 The source code and more information is available at [http://tda.gatech.edu/software/  
 552 dagP/](http://tda.gatech.edu/software/dagP/).

553 We have performed an extensive evaluation of the proposed multilevel directed

| Graph      | Parameters                      | <i>#vertex</i> | <i>#edge</i> | max. deg. | avg. deg. | <i>#source</i> | <i>#target</i> |
|------------|---------------------------------|----------------|--------------|-----------|-----------|----------------|----------------|
| 2mm        | P=10, Q=20, R=30,<br>S=40       | 36,500         | 62,200       | 40        | 1.704     | 2100           | 400            |
| 3mm        | P=10, Q=20, R=30,<br>S=40, T=50 | 111,900        | 214,600      | 40        | 1.918     | 3900           | 400            |
| adi        | T=20, N=30                      | 596,695        | 1,059,590    | 109,760   | 1.776     | 843            | 28             |
| atax       | M=210, N=230                    | 241,730        | 385,960      | 230       | 1.597     | 48530          | 230            |
| covariance | M=50, N=70                      | 191,600        | 368,775      | 70        | 1.925     | 4775           | 1275           |
| doitgen    | P=10, Q=15, R=20                | 123,400        | 237,000      | 150       | 1.921     | 3400           | 3000           |
| durbin     | N=250                           | 126,246        | 250,993      | 252       | 1.988     | 250            | 249            |
| fdtd-2d    | T=20, X=30, Y=40                | 256,479        | 436,580      | 60        | 1.702     | 3579           | 1199           |
| gemm       | P=60, Q=70, R=80                | 1,026,800      | 1,684,200    | 70        | 1.640     | 14600          | 4200           |
| gemver     | N=120                           | 159,480        | 259,440      | 120       | 1.627     | 15360          | 120            |
| gesummv    | N=250                           | 376,000        | 500,500      | 500       | 1.331     | 125250         | 250            |
| heat-3d    | T=40, N=20                      | 308,480        | 491,520      | 20        | 1.593     | 1280           | 512            |
| jacobi-1d  | T=100, N=400                    | 239,202        | 398,000      | 100       | 1.664     | 402            | 398            |
| jacobi-2d  | T=20, N=30                      | 157,808        | 282,240      | 20        | 1.789     | 1008           | 784            |
| lu         | N=80                            | 344,520        | 676,240      | 79        | 1.963     | 6400           | 1              |
| ludcmp     | N=80                            | 357,320        | 701,680      | 80        | 1.964     | 6480           | 1              |
| mvt        | N=200                           | 200,800        | 320,000      | 200       | 1.594     | 40800          | 400            |
| seidel-2d  | M=20, N=40                      | 261,520        | 490,960      | 60        | 1.877     | 1600           | 1              |
| symm       | M=40, N=60                      | 254,020        | 440,400      | 120       | 1.734     | 5680           | 2400           |
| syr2k      | M=20, N=30                      | 111,000        | 180,900      | 60        | 1.630     | 2100           | 900            |
| syrk       | M=60, N=80                      | 594,480        | 975,240      | 81        | 1.640     | 8040           | 3240           |
| trisolv    | N=400                           | 240,600        | 320,000      | 399       | 1.330     | 80600          | 1              |
| trmm       | M=60, N=80                      | 294,570        | 571,200      | 80        | 1.939     | 6570           | 4800           |

Table 5.1: Instances from the Polyhedral Benchmark suite (PolyBench).

554 acyclic graph partitioning method on DAG instances coming from two sources. The  
555 first set of instances is from the Polyhedral Benchmark suite (PolyBench) [26], whose  
556 parameters are listed in Table 5.1. The graphs in the Polyhedral Benchmark suite  
557 arise from various linear computation kernels. The parameters in the second column  
558 of Table 5.1 represent the size of these computation kernels. For more details, we re-  
559 fer the reader to the description of the Polyhedral Benchmark suite (PolyBench) [26].  
560 The second set of instances is obtained from the matrices available in the SuiteS-  
561 parse Matrix Collection (formerly known as the University of Florida Sparse Matrix  
562 Collection) [8]. From this collection, we pick all the matrices satisfying the following  
563 properties: listed as binary, square, and has at least 100000 rows and at most  $2^{26}$   
564 nonzeros. There were a total of 95 matrices at the time of experimentation, where  
565 two matrices (ids 1514 and 2294) having the same pattern. We discard the duplicate  
566 and use the remaining 94 matrices for experiments. For each such matrix, we take  
567 the strict upper triangular part as the associated DAG instance, whenever this part  
568 has more nonzeros than the lower triangular part; otherwise we take the strict lower  
569 triangular part. All edges have unit cost, and all vertices have unit weight.

570 Since the proposed heuristics have a randomized behavior (the traversals used  
571 in the coarsening and refinement heuristics are randomized), we run them 10 times  
572 for each DAG instance, and report the averages of these runs. We use performance  
573 profiles [9] to present the edge-cut results. A performance profile plot shows the  
574 probability that a specific method gives results within a factor  $\theta$  of the best edge cut  
575 obtained by any of the methods compared in the plot. Hence, the higher and closer  
576 a plot to the  $y$ -axis, the better the method is.

577 We set the load imbalance parameter  $\varepsilon = 0.03$  in (2.1) for all experiments. The  
578 vertices are unit weighted, therefore, the imbalance is rarely an issue for a move-based  
579 partitioner.

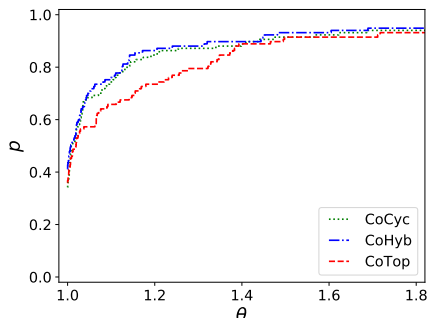


Fig. 5.1: Performance profiles of the proposed multilevel algorithm variants using three different coarsening heuristics in terms of edge cut.

580 **5.1. Coarsening evaluation.** We first evaluate the proposed coarsening heuristics.  
 581 The aim is to find an effective one to set as a default coarsening heuristic.

582 The performance profile chart given in Figure 5.1 shows the effect of the coarsening  
 583 heuristics on the final edge cut for the whole dataset. The variants of the proposed  
 584 multilevel algorithm which use different coarsening schemes are named as CoTop (Sec-  
 585 tion 4.1.1), CoCyc (Section 4.1.2), and CoHyb (Section 4.1.3). Here, and in the rest of  
 586 the paper, we used a randomized Depth-First topological order for the node traversal  
 587 in the coarsening heuristics, since it performed better in practice. In Figure 5.1, we  
 588 see that CoCyc and CoHyb behave similarly; this is expected as not all graphs have  
 589 vertices with large degrees. From this figure, we conclude that in general, the coarsening  
 590 heuristics CoHyb and CoCyc are more helpful than CoTop in reducing the edge  
 591 cut.

592 Another important characteristic to assess for a coarsening heuristic is its con-  
 593 traction efficiency. It is important that the coarsening phase does not stop too early  
 594 and that the coarsest graph is small enough to be partitioned efficiently. Table 5.2  
 595 gives the maximum, the average, and the standard deviation of vertex and edge weight  
 596 ratios, and the average, the minimum, and the maximum number of coarsening levels  
 597 observed for the two datasets. An effective coarsening heuristic should have small  
 598 vertex and edge weight ratios. We see that CoCyc and CoHyb behave similarly and  
 599 provide slightly better results than CoTop on both datasets. The graphs from the two  
 600 datasets have different characteristics. All coarsening heuristics perform better on the  
 601 PolyBench instances compared to the UFL instances: they obtain smaller ratios in  
 602 the number of remaining vertices, and yield smaller edge weights. Furthermore, the  
 603 maximum vertex and edge weight ratios are smaller in PolyBench instances, again  
 604 with all coarsening methods. To the best of our understanding, these happen due to  
 605 two reasons; (i) the average degree in the UFL instances is larger than that of the  
 606 PolyBench instances (3.63 vs. 1.72); (ii) the ratio of the total number of source and  
 607 target vertices to the total number of vertices is again larger in the UFL instances  
 608 (0.13 vs. 0.03). Based on Figure 5.1 and Table 5.2, we set CoHyb as the default  
 609 coarsening heuristic, as it performs better than CoTop in terms of final edge cut, and  
 610 is guaranteed to be more efficient than CoCyc in terms of run time.

611 **5.2. Constraint coarsening and initial partitioning.** We now investigate  
 612 the effect of using undirected graph partitioners to obtain a more effective coarsen-

| Algorithm | Vertex ratio (%) |          |       | Edge weight ratio (%) |          |       | Coarsening levels |     |      |
|-----------|------------------|----------|-------|-----------------------|----------|-------|-------------------|-----|------|
|           | avg              | std. dev | max   | avg                   | std. dev | max   | avg               | min | max  |
| CoTop     | 1.29             | 6.34     | 46.72 | 26.07                 | 24.95    | 87.00 | 12.45             | 2   | 17.0 |
| CoCyc     | 1.06             | 6.31     | 47.29 | 25.97                 | 24.86    | 87.90 | 12.74             | 2   | 17.6 |
| CoHyb     | 1.08             | 6.27     | 46.70 | 26.00                 | 24.80    | 87.00 | 12.69             | 2   | 17.7 |
| CoTop     | 1.33             | 2.26     | 8.50  | 25.67                 | 11.08    | 47.60 | 7.44              | 4   | 11.8 |
| CoCyc     | 0.41             | 0.90     | 4.10  | 24.96                 | 9.20     | 37.00 | 8.37              | 5   | 12.0 |
| CoHyb     | 0.54             | 0.88     | 3.60  | 24.81                 | 9.33     | 39.00 | 8.46              | 5   | 11.9 |

Table 5.2: The maximum, average, and standard deviation of vertex and edge weight ratios, and the average, the minimum, and the maximum number of coarsening levels for the UFL dataset on the upper half of the table, and for the PolyBench dataset on the lower half.

ing and better initial partitions as explained in [Subsection 4.4](#). We compare three variants of the proposed multilevel scheme. All of them use the refinement described in [Subsection 4.3](#) in the uncoarsening phase.

- **CoHyb**: this variant uses the hybrid coarsening heuristic described in [Section 4.1.3](#) and the greedy directed graph growing heuristic described in [Section 4.2.1](#) in the initial partitioning phase. This method does not use constraint coarsening.
- **CoHyb\_C**: this variant uses an acyclic partition of the finest graph obtained as outlined in [Section 4.2.2](#) to guide the hybrid coarsening heuristic described in [Subsection 4.4](#), and uses the greedy directed graph growing heuristic in the initial partitioning phase.
- **CoHyb\_CIP**: this variant uses the same constraint coarsening heuristic as the previous method, but inherits the fixed acyclic partition of the finest graph as the initial partitioning.

The comparison of these three variants are given in [Figure 5.2](#) for the whole dataset. From [Figure 5.2](#), we see that using the constraint coarsening is always helpful with respect to not using them. This clearly separates **CoHyb\_C** and **CoHyb\_CIP** from **CoHyb** after  $\theta = 1.1$ . Furthermore, applying the constraint initial partitioning (on top of the constraint coarsening) brings tangible improvements.

In the light of the experiments presented here, we suggest the variant **CoHyb\_CIP** for general problem instances, as this has clear advantages over others in our dataset.

**5.3. Evaluating CoHyb\_CIP with respect to a single level algorithm.** We compare **CoHyb\_CIP** (the variant of the proposed approach with constraint coarsening and initial partitioning) with a single-level algorithm that uses an undirected graph partitioning, fixes the acyclicity, and refines the partitions. This last variant is denoted as **UndirFix**, and it is the algorithm described in [Section 4.2.2](#). Both variants use the same initial partitioning approach, which utilizes MeTiS [16] as the undirected partitioner. The difference between **UndirFix** and **CoHyb\_CIP** is the latter’s ability to refine the initial partition at multiple levels. [Figure 5.3](#) presents this comparison. The plots show that the multilevel scheme **CoHyb\_CIP** outperforms the single level scheme **UndirFix** at all appropriate ranges of  $\theta$ , attesting to the importance of the multilevel scheme.

**5.4. Comparison with existing work.** Here we compare our approach with the evolutionary graph partitioning approach developed by Moreira et al. [21], and

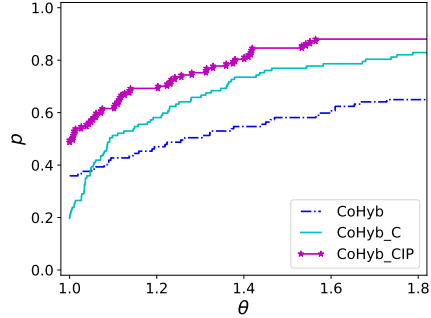


Fig. 5.2: Performance profiles for the edge cut obtained by the proposed multilevel algorithm using the constraint coarsening and partitioning (CoHyb\_CIP), using the constraint coarsening and the greedy directed graph growing (CoHyb\_C), and the best identified approach without constraints (CoHyb).

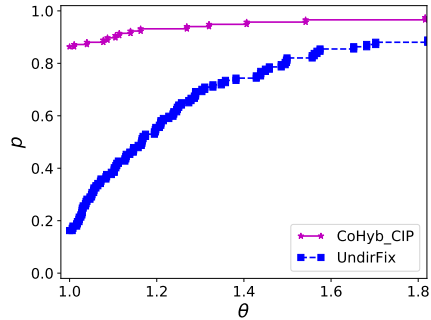


Fig. 5.3: Performance profiles for the edge cut obtained by the proposed multilevel approach using the constraint coarsening and partitioning (CoHyb\_CIP) and using the same approach without coarsening (UndirFix).

647 briefly with our previous work [15].

648 Figure 5.4 shows how CoHyb\_CIP and CoTop compare with the evolutionary ap-  
 649 proach in terms of the edge cut on the 23 graphs of the PolyBench dataset, for the  
 650 number of partitions  $k \in \{2, 4, 8, 16, 32\}$ . We use the average edge cut value of 10  
 651 runs for CoTop and CoHyb\_CIP and the average values presented in [21] for the evolu-  
 652 tionary algorithm. As seen in the figure, the CoTop variant of the proposed multilevel  
 653 approach obtains the best results on this specific dataset (all variants of the proposed  
 654 approach outperform the evolutionary approach).

655 Tables A.1 and A.2 show the average and best edge cuts found by CoHyb\_CIP and  
 656 CoTop variants of our partitioner and the evolutionary approach on the PolyBench  
 657 dataset. The two tables just after them (Tables A.3 and A.4) give the associated  
 658 balance factors. The variants CoHyb\_CIP and CoTop of the proposed algorithm obtain  
 659 strictly better results than the evolutionary approach in 78 and 75 instances (out of  
 660 115), respectively, when the average edge cuts are compared.



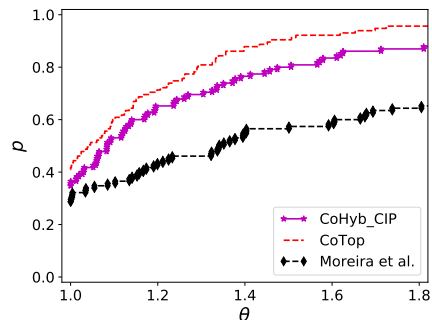


Fig. 5.4: Performance profiles for the edge cut obtained by CoHyb\_CIP, CoTop, and Moreira et al.’s approach on the PolyBench dataset with  $k \in \{2, 4, 8, 16, 32\}$ .

661 As seen in the last row of Table A.2, CoHyb\_CIP obtains 26% less edge cut than  
 662 the evolutionary approach on average (geometric mean) when the average cuts are  
 663 compared (0.74 vs. 1.00 in the table); when the best cuts are compared, CoHyb\_CIP  
 664 obtains 48% less edge cut (0.50 vs. 0.96). Moreover, CoTop obtains 37% less edge cut  
 665 than the evolutionary approach when the average cuts are compared (0.63 vs. 1.00  
 666 in the table); when the best cuts are compared, CoTop obtains 41% less cut (0.57  
 667 vs. 0.96). In some instances (for example `covariance` and `gemm` in Table A.1 and  
 668 `syrc` and `trmm` in Table A.2), we see large differences between the average and the  
 669 best results of CoTop and CoHyb\_CIP. Combined with the observation that CoHyb\_CIP  
 670 yields better results in general, this suggests that the neighborhood structure can be  
 671 improved (see the notion of the strength of a neighborhood [24, Section 19.6]). All  
 672 partitions attain 3% balance.

673 The proposed approach with all the reported variants take about 30 minutes to  
 674 complete the whole set of experiments for this dataset, whereas the evolutionary ap-  
 675 proach is much more compute-intensive, as it has to run the multilevel partitioning  
 676 algorithm numerous times to create and update the population of partitions for the  
 677 evolutionary algorithm. The multilevel approach of Moreira et al. [21] is more compa-  
 678 rable in terms of characteristics with our multilevel scheme. When we compare CoTop  
 679 with the results of the multilevel algorithm by Moreira et al., our approach provides  
 680 results that are 37% better on average and CoHyb\_CIP approach provides results that  
 681 are 26% better on average, highlighting the fact that keeping the acyclicity of the  
 682 directed graph through the multilevel process is useful.

683 Finally, CoTop and CoHyb\_CIP also outperform the previous version of our mul-  
 684 tilevel partitioner [15], which is based on a direct  $k$ -way partitioning scheme and  
 685 matching heuristics for the coarsening phase, by 45% and 35% on average, respec-  
 686 tively, on the same dataset.

687 **5.5. Single commodity flow-like problem instances.** In many of the in-  
 688 stances of our dataset, graphs have many source and target vertices. We investigate  
 689 how our algorithm performs on problems where all source vertices should be in a given  
 690 part, and all target vertices should be in the other part, while also achieving balance.  
 691 This is a problem close to the maximum flow problem, where we want to find the  
 692 maximum flow (or minimum cut) from the sources to the targets with balance on  
 693 part weights. Furthermore, addressing this problem also provides a setting for solving

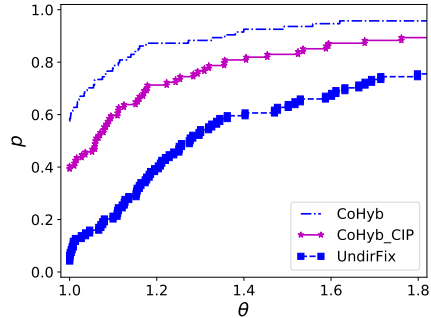


Fig. 5.5: Performance profiles of CoHyb, CoHyb\_CIP and UndirFix in terms of edge cut for single source, single target graph dataset. The average of 5 runs are reported for each approach.

694 partitioning problems with fixed vertices.

695 For these experiments, we used the UFL dataset. We discarded all isolated ver-  
 696 tices, added to each graph a source vertex  $S$  (with an edge from  $S$  to all source vertices  
 697 of the original graph with a cost equal to the number of edges) and target vertex  $T$   
 698 (with an edge from all target vertices of the original graph to  $T$  with a cost equal  
 699 to the number of edges). A feasible partition should avoid cutting these edges, and  
 700 separate all sources from the targets.

701 The performance profiles of CoHyb, CoHyb\_CIP and UndirFix are given in Fig-  
 702 ure 5.5 with the edge cut as the evaluation criterion. As seen in this figure, CoHyb  
 703 is the best performing variant, and UndirFix is the worst performing variant. This is  
 704 interesting as in the general setting, we saw a reverse relation. The variant CoHyb\_CIP  
 705 performs in the middle, as it combines the other two.

706 **5.6. Runtime performance.** We now assess the runtime performance of the  
 707 proposed algorithms. Figure 5.6 shows the runtime comparison and distribution for  
 708 13 graphs with the longest coarsening time for the CoTop variant. A description of  
 709 these 13 graphs can be found in Table 5.3. In Figure 5.6, each graph has three bars  
 710 representing the runtime for the multilevel algorithm using the coarsening heuristics  
 711 described in Subsection 4.1: CoTop, CoCyc, and CoHyb. We can see that the run time  
 712 performance of the three coarsening heuristics are similar. This means that, the cycle  
 713 detection function in CoCyc does not introduce a large overhead, as stated in Sec-  
 714 tion 4.1.2. Most of the time, CoCyc has a bit longer run time than CoTop, and CoHyb  
 715 offers a good tradeoff. Note that in Figure 5.6, the computation time of the initial  
 716 partitioning is negligible compared to that of the coarsening and uncoarsening phases,  
 717 which means that the graphs have been efficiently contracted during the coarsening  
 718 phase.

719 Figure 5.7 shows the comparison of the five variants of the proposed multilevel  
 720 scheme and the single level scheme on the whole dataset. Each algorithm is run 10  
 721 times on each graph. As expected, CoTop offers the best performance, and CoHyb  
 722 offers a good trade-off between CoTop and CoCyc. An interesting remark is that these  
 723 three algorithms have a better run time than the single level algorithm UndirFix. For  
 724 example, on the average, CoTop is 1.44 times faster than UndirFix. This is mainly due  
 725 to cost of fixing acyclicity. Undirected partitioning accounts for roughly 25% of the

| Graph              | #vertex    | #edge      | Max In | Max Out | Avg Deg | #source   | #target   |
|--------------------|------------|------------|--------|---------|---------|-----------|-----------|
| 333SP              | 3,712,815  | 11,108,633 | 9      | 27      | 2.992   | 188,112   | 316,151   |
| AS365              | 3,799,275  | 11,368,076 | 10     | 13      | 2.992   | 306,791   | 519,431   |
| M6                 | 3,501,776  | 10,501,936 | 10     | 10      | 2.999   | 280,784   | 472,230   |
| cit-Patents        | 3,774,768  | 16,518,209 | 779    | 770     | 4.376   | 515,980   | 1,685,419 |
| delaunay-n22       | 4,194,304  | 12,582,869 | 15     | 17      | 3       | 555,807   | 337,743   |
| hugebubbles-00010  | 19,458,087 | 29,179,764 | 3      | 3       | 1.5     | 3,355,886 | 3,054,827 |
| hugetrace-00020    | 16,002,413 | 23,998,813 | 3      | 3       | 1.5     | 2,514,461 | 2,407,017 |
| hugetric-00010     | 6,592,765  | 9,885,854  | 3      | 3       | 1.5     | 1,085,866 | 1,006,163 |
| italy-osm          | 6,686,493  | 7,013,978  | 5      | 8       | 1.049   | 155,509   | 458,561   |
| rgg-n-2-22-s0      | 4,194,304  | 30,359,198 | 24     | 25      | 7.238   | 3,550     | 3,576     |
| road-usa           | 23,947,347 | 28,854,312 | 8      | 8       | 1.205   | 6,392,288 | 8,010,032 |
| wb-edu             | 9,845,725  | 29,494,732 | 17,489 | 3841    | 2.996   | 1,489,057 | 2,794,680 |
| wikipedia-20060925 | 2,983,494  | 26,103,626 | 74,970 | 5,844   | 8.749   | 1,406,429 | 72,744    |

Table 5.3: 13 instances from the UFL dataset with the longest coarsening times for CoTop.

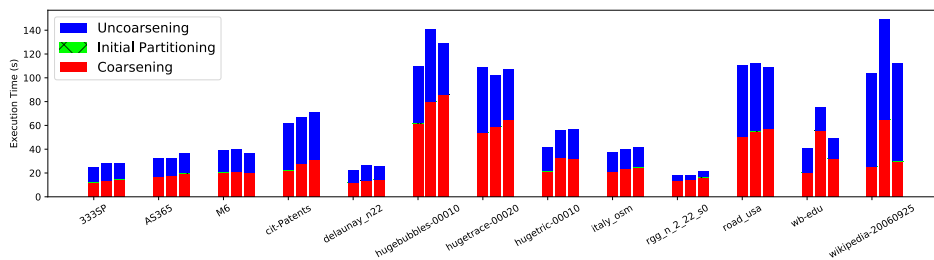


Fig. 5.6: Runtimes for CoTop, CoCyc, and CoHyb variants of the proposed multilevel scheme. For each bar group, the first, second, and the third bar present the detailed runtimes of CoTop, CoCyc, and CoHyb, respectively.

726 execution time of `UndirFix`, and fixing the acyclicity constitutes the remaining 75%.  
 727 Finally, the variants of the multilevel algorithm using constraint coarsening heuristics  
 728 provide satisfying run time performance with respect to the others.

729 **6. Conclusion.** We proposed a multilevel approach for acyclic partitioning of  
 730 directed acyclic graphs. This problem is close to the standard graph partitioning in  
 731 that the aim is to partition the vertices into a number of parts while minimizing the  
 732 edge cut and meeting a balance criterion on the part weights. Unlike the standard  
 733 graph partitioning problem, the directions of the edges are important and the resulting  
 734 partitions should have acyclic dependencies.

735 We proposed coarsening, initial partitioning, and refinement heuristics for the  
 736 target problem. The proposed heuristics take the directions of the edges into account  
 737 and maintain the acyclicity through all the multilevel hierarchy. We also proposed  
 738 efficient and effective approaches to use the standard undirected graph partitioning  
 739 tools in the multilevel scheme for coarsening and initial partitioning. We performed  
 740 a large set of experiments on a dataset with graphs having different characteristics  
 741 and evaluated different combinations of the proposed heuristics. Our experiments  
 742 suggested (i) the use of constraint coarsening and initial partitioning, where the main  
 743 coarsening heuristic is a hybrid one which avoids the cycles, and in case it does not,  
 744 performs a fast cycle detection (`CoHyb_CIP`) for the general case; (ii) a pure multilevel

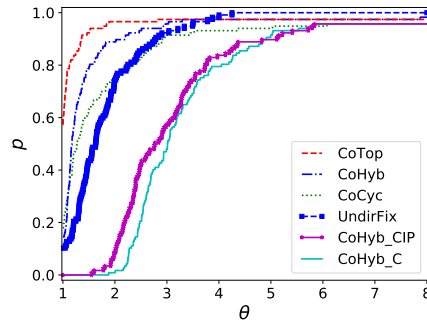


Fig. 5.7: Runtime performance profile of CoCyc, CoHyb, CoTop, CoHyb\_C, CoHyb\_CIP and UndirFix on the whole dataset. The values are the averages of 10 runs.

745 scheme without constraint coarsening, using the hybrid coarsening heuristic (CoHyb)  
 746 for the cases where a number of sources need to be separated from a number of targets;  
 747 (iii) a pure multilevel scheme without constraint coarsening, using the fast coarsening  
 748 algorithm (CoTop) for the cases where the degrees of the vertices are small. All three  
 749 approaches are shown to be more effective and efficient than the current state of the  
 750 art.

751 An avenue for the future work is applying the proposed multilevel scheme in real  
 752 life applications that are based on task-graphs. This requires a scheduling step to be  
 753 applied after the proposed partitioning scheme, which needs further investigations. A  
 754 recent work uses a multilevel algorithm for recombination and mutation [22]. Plugging  
 755 in our multilevel scheme to that framework can yield significant improvements.

756 **Acknowledgment.** We thank John Gilbert for his comments on an earlier ver-  
 757 sion of this work presented at CSC'16. John suggested that we look at the spiral  
 758 ordering of the grid graph.

759

## REFERENCES

- 760 [1] K. AGRAWAL, J. T. FINEMAN, J. KRAGE, C. E. LEISERSON, AND S. TOLEDO, *Cache-conscious*  
 761 *scheduling of streaming applications*, in Proc. Twenty-fourth Annual ACM Symposium on  
 762 *Parallelism in Algorithms and Architectures*, SPAA '12, New York, NY, USA, 2012, ACM,  
 763 pp. 236–245.
- 764 [2] T. N. BUI AND C. JONES, *A heuristic for reducing fill-in in sparse matrix factorization*, in Proc.  
 765 *6th SIAM Conf. Parallel Processing for Scientific Computing*, SIAM, 1993, pp. 445–452.
- 766 [3] Ü. V. ÇATALYÜREK AND C. AYKANAT, *PaToH: A Multilevel Hypergraph Partitioning Tool*,  
 767 *Version 3.0*, Bilkent University, Dept. Comp. Engineering, Ankara, 06533 Turkey. PaToH  
 768 is available at <http://cc.gatech.edu/~umit/software.html>, 1999.
- 769 [4] T. F. COLEMAN AND W. XU, *Parallelism in structured Newton computations*, in *Parallel*  
 770 *Computing: Architectures, Algorithms and Applications*, ParCo 2007, Forschungszentrum  
 771 Jülich and RWTH Aachen University, Germany, 2007, pp. 295–302.
- 772 [5] T. F. COLEMAN AND W. XU, *Fast (structured) Newton computations*, *SIAM Journal on Scien-*  
 773 *tific Computing*, 31 (2009), pp. 1175–1191.
- 774 [6] T. F. COLEMAN AND W. XU, *Automatic Differentiation in MATLAB using ADMAT with*  
 775 *Applications*, SIAM, 2016.
- 776 [7] J. CONG, Z. LI, AND R. BAGRODIA, *Acyclic multi-way partitioning of Boolean networks*, in  
 777 *Proceedings of the 31st Annual Design Automation Conference*, DAC'94, New York, NY,  
 778 USA, 1994, ACM, pp. 670–675.
- 779 [8] T. A. DAVIS AND Y. HU, *The University of Florida sparse matrix collection*, *ACM Trans. Math.*

- 780           Softw., 38 (2011), pp. 1:1–1:25.
- 781 [9] E. D. DOLAN AND J. J. MORÉ, *Benchmarking optimization software with performance profiles*,  
782           Mathematical programming, 91 (2002), pp. 201–213.
- 783 [10] V. ELANGO, F. RASTELLO, L.-N. POUCHET, J. RAMANUJAM, AND P. SADAYAPPAN, *On charac-*  
784           *terizing the data access complexity of programs*, SIGPLAN Not., 50 (2015), pp. 567–580.
- 785 [11] N. FAUZIA, V. ELANGO, M. RAVISHANKAR, J. RAMANUJAM, F. RASTELLO, A. ROUNTEV, L.-N.  
786           POUCHET, AND P. SADAYAPPAN, *Beyond reuse distance analysis: Dynamic analysis for*  
787           *characterization of data locality potential*, ACM Trans. Archit. Code Optim., 10 (2013),  
788           pp. 53:1–53:29.
- 789 [12] C. M. FIDUCCIA AND R. M. MATTHEYSES, *A linear-time heuristic for improving network par-*  
790           *titions*, in Design Automation, 1982. 19th Conference on, IEEE, 1982, pp. 175–181.
- 791 [13] M. R. GAREY AND D. S. JOHNSON, *Computers and Intractability: A Guide to the Theory of*  
792           *NP-Completeness*, W. H. Freeman & Co., New York, NY, USA, 1979.
- 793 [14] B. HENDRICKSON AND R. LELAND, *The Chaco user’s guide, version 1.0*, Tech. Report SAND93–  
794           2339, Sandia National Laboratories, Albuquerque, NM, October 1993.
- 795 [15] J. HERRMANN, J. KHO, B. UÇAR, K. KAYA, AND Ü. V. ÇATALYÜREK, *Acyclic partitioning of*  
796           *large directed acyclic graphs*, in Proceedings of the 17th IEEE/ACM International Sym-  
797           posium on Cluster, Cloud and Grid Computing, CCGRID, Madrid, Spain, May 2017,  
798           pp. 371–380.
- 799 [16] G. KARYPIS AND V. KUMAR, *MeTiS: A Software Package for Partitioning Unstructured*  
800           *Graphs, Partitioning Meshes, and Computing Fill-Reducing Orderings of Sparse Matrices*  
801           *Version 4.0*, University of Minnesota, Department of Comp. Sci. and Eng., Army HPC  
802           Research Cent., Minneapolis, 1998.
- 803 [17] B. W. KERNIGHAN, *Optimal sequential partitions of graphs*, J. ACM, 18 (1971), pp. 34–40.
- 804 [18] B. W. KERNIGHAN AND S. LIN, *An efficient heuristic procedure for partitioning graphs*, The  
805           Bell System Technical Journal, 49 (1970), pp. 291–307.
- 806 [19] M. R. B. KRISTENSEN, S. A. F. LUND, T. BLUM, AND J. AVERY, *Fusion of parallel array*  
807           *operations*, in Proceedings of the 2016 International Conference on Parallel Architectures  
808           and Compilation, New York, NY, USA, 2016, ACM, pp. 71–85.
- 809 [20] M. R. B. KRISTENSEN, S. A. F. LUND, T. BLUM, K. SKOVHEDE, AND B. VINTER, *Bohrium: A*  
810           *virtual machine approach to portable parallelism*, in Proceedings of the 2014 IEEE Inter-  
811           national Parallel & Distributed Processing Symposium Workshops, IPDPSW ’14, Wash-  
812           ington, DC, USA, 2014, IEEE Computer Society, pp. 312–321.
- 813 [21] O. MOREIRA, M. POPP, AND C. SCHULZ, *Graph partitioning with acyclicity constraints*, in 16th  
814           International Symposium on Experimental Algorithms, SEA, London, UK, 2017, Schloss  
815           Dagstuhl–Leibniz-Zentrum fuer Informatik.
- 816 [22] O. MOREIRA, M. POPP, AND C. SCHULZ, *Evolutionary multi-level acyclic graph partitioning*, in  
817           Proceedings of the Genetic and Evolutionary Computation Conference, GECCO, Kyoto,  
818           Japan, 2018, ACM, pp. 332–339.
- 819 [23] J. NOSSACK AND E. PESCH, *A branch-and-bound algorithm for the acyclic partitioning problem*,  
820           Computers & Operations Research, 41 (2014), pp. 174–184.
- 821 [24] C. H. PAPADIMITRIOU AND K. STEIGLITZ, *Combinatorial Optimization: Algorithms and Com-*  
822           *plexity*, Dover Publications, (Corrected, unabridged reprint of Combinatorial Optimization:  
823           Algorithms and Complexity originally published by Prentice-Hall Inc., New Jersey, 1982),  
824           New York, 1998.
- 825 [25] F. PELLEGRINI, *SCOTCH 5.1 User’s Guide*, Laboratoire Bordelais de Recherche en Informa-  
826           tique (LaBRI), 2008.
- 827 [26] L.-N. POUCHET, *Polybench: The polyhedral benchmark suite*, URL: [http://web.cse.ohio-](http://web.cse.ohio-state.edu/pouchet/software/polybench/)  
828           state.edu/pouchet/software/polybench/, (2012).
- 829 [27] P. SANDERS AND C. SCHULZ, *Engineering multilevel graph partitioning algorithms*, in Algo-  
830           rithms – ESA 2011: 19th Annual European Symposium, Saarbrücken, Germany, Septem-  
831           ber 5-9, 2011. Proceedings, C. Demetrescu and M. M. Halldórsson, eds., Berlin, Heidelberg,  
832           2011, Springer Berlin Heidelberg, pp. 469–480.
- 833 [28] C. WALSHAW, *Multilevel refinement for combinatorial optimisation problems*, Annals of Oper-  
834           ations Research, 131 (2004), pp. 325–372.
- 835 [29] E. S. H. WONG, E. F. Y. YOUNG, AND W. K. MAK, *Clustering based acyclic multi-way parti-*  
836           *tioning*, in Proceedings of the 13th ACM Great Lakes Symposium on VLSI, GLSVLSI ’03,  
837           New York, NY, USA, 2003, ACM, pp. 203–206.

838           **Appendix A. Detailed results on the PolyBench instances.** We give in  
839 Tables A.1 and A.2 the detailed edge cut results of the proposed CoTop, CoHyb\_CIP and

840 of Moreira et al.'s evolutionary algorithm [21]. Tables A.3 and A.4 give the balance  
841 attained in the partitions. In these two tables, the average balance of the ten runs  
842 yielding the average edge cut of Tables A.1 and A.2 is reported per problem instance.  
843 The balance of the partition yielding the best edge cut of the previous tables is also  
844 given per problem instance.



| Graph      | k  | Moreira et al. [21] |        | CoHyb_CIP |        | CoTop   |        |
|------------|----|---------------------|--------|-----------|--------|---------|--------|
|            |    | Average             | Best   | Average   | Best   | Average | Best   |
| 2mm        | 2  | 200                 | 200    | 200       | 200    | 200     | 200    |
|            | 4  | 947                 | 930    | 6134      | 2686   | 2160    | 1900   |
|            | 8  | 7181                | 6604   | 8713      | 6300   | 5361    | 4027   |
|            | 16 | 13330               | 13092  | 12135     | 9380   | 11196   | 10698  |
|            | 32 | 14583               | 14321  | 15911     | 14829  | 15932   | 14838  |
| 3mm        | 2  | 1000                | 1000   | 7399      | 800    | 1000    | 1000   |
|            | 4  | 38722               | 37899  | 16771     | 7653   | 9264    | 8634   |
|            | 8  | 58129               | 49559  | 24330     | 9832   | 28121   | 24270  |
|            | 16 | 64384               | 60127  | 37041     | 31036  | 39683   | 37194  |
|            | 32 | 62279               | 58190  | 46437     | 43062  | 48567   | 43210  |
| adi        | 2  | 134945              | 134675 | 142719    | 142174 | 143067  | 139672 |
|            | 4  | 284666              | 283892 | 212938    | 211939 | 215399  | 214945 |
|            | 8  | 290823              | 290672 | 271949    | 266349 | 256302  | 255522 |
|            | 16 | 326963              | 326923 | 300755    | 292351 | 282485  | 281511 |
|            | 32 | 370876              | 370413 | 324494    | 316241 | 306075  | 305411 |
| atax       | 2  | 47826               | 47424  | 44942     | 38679  | 39876   | 39876  |
|            | 4  | 82397               | 76245  | 60187     | 47184  | 48645   | 48645  |
|            | 8  | 113410              | 111051 | 63353     | 51580  | 51243   | 50419  |
|            | 16 | 127687              | 125146 | 70723     | 62697  | 59208   | 57085  |
|            | 32 | 132092              | 130854 | 78264     | 67401  | 69556   | 63166  |
| covariance | 2  | 66520               | 66445  | 27269     | 4775   | 55195   | 17183  |
|            | 4  | 84626               | 84213  | 82125     | 61793  | 61991   | 34307  |
|            | 8  | 103710              | 102425 | 136946    | 122656 | 74325   | 50680  |
|            | 16 | 125816              | 123276 | 142177    | 123221 | 119284  | 106422 |
|            | 32 | 142214              | 137905 | 121155    | 103751 | 133522  | 117431 |
| doitgen    | 2  | 43807               | 42208  | 5035      | 3000   | 5947    | 5947   |
|            | 4  | 72115               | 71072  | 37767     | 22290  | 37051   | 31157  |
|            | 8  | 76977               | 75114  | 51283     | 43572  | 53244   | 50795  |
|            | 16 | 84203               | 77436  | 62296     | 56650  | 66483   | 64488  |
|            | 32 | 94135               | 92739  | 68350     | 62576  | 74786   | 70168  |
| durbin     | 2  | 12997               | 12997  | 12997     | 12997  | 12997   | 12997  |
|            | 4  | 21641               | 21641  | 21572     | 21572  | 21566   | 21566  |
|            | 8  | 27571               | 27571  | 27519     | 27518  | 27520   | 27520  |
|            | 16 | 32865               | 32865  | 32852     | 32848  | 32912   | 32912  |
|            | 32 | 39726               | 39725  | 39738     | 39732  | 39826   | 39826  |
| fdtd-2d    | 2  | 5494                | 5494   | 6264      | 6003   | 6024    | 5896   |
|            | 4  | 15100               | 15099  | 15294     | 13199  | 16965   | 16674  |
|            | 8  | 33087               | 32355  | 23699     | 21886  | 35711   | 34361  |
|            | 16 | 35714               | 35239  | 32917     | 30725  | 44643   | 43608  |
|            | 32 | 43961               | 42507  | 42515     | 41258  | 53658   | 52420  |
| gemm       | 2  | 383084              | 382433 | 4200      | 4200   | 44549   | 44549  |
|            | 4  | 507250              | 500526 | 168962    | 12600  | 59854   | 46677  |
|            | 8  | 578951              | 575004 | 183228    | 36273  | 116990  | 96059  |
|            | 16 | 615342              | 613373 | 294777    | 241136 | 263050  | 238125 |
|            | 32 | 626472              | 623271 | 330937    | 307225 | 332946  | 299774 |
| gemver     | 2  | 29349               | 29270  | 26368     | 22824  | 20913   | 20913  |
|            | 4  | 49361               | 49229  | 45689     | 38663  | 40299   | 40185  |
|            | 8  | 68163               | 67094  | 56930     | 49776  | 55266   | 53759  |
|            | 16 | 78115               | 75596  | 62143     | 57779  | 59072   | 56598  |
|            | 32 | 85331               | 84865  | 75425     | 68673  | 73131   | 71349  |
| gesummv    | 2  | 1666                | 500    | 24762     | 500    | 500     | 500    |
|            | 4  | 98542               | 94493  | 24613     | 1783   | 10316   | 8710   |
|            | 8  | 101533              | 98982  | 25342     | 13522  | 9618    | 9397   |
|            | 16 | 112064              | 104866 | 37819     | 21155  | 35686   | 30954  |
|            | 32 | 117752              | 114812 | 48775     | 42523  | 45050   | 40671  |
| heat-3d    | 2  | 8695                | 8684   | 10165     | 9648   | 9378    | 9225   |
|            | 4  | 14592               | 14592  | 17093     | 16321  | 16700   | 16424  |
|            | 8  | 20608               | 20608  | 28388     | 25862  | 25883   | 25470  |
|            | 16 | 31615               | 31500  | 47612     | 46825  | 42137   | 41261  |
|            | 32 | 51963               | 50758  | 64614     | 62894  | 70462   | 69439  |

Table A.1: Comparing the edge cuts obtained by CoHyb\_CIP and CoTop with those obtained by the evolutionary algorithm of Moreira et al. on the Polyhedral Benchmark Suite (first set of results).

| Graph          | $k$ | Moreira et al. [21] |        | CoHyb_CIP |        | CoTop   |        |
|----------------|-----|---------------------|--------|-----------|--------|---------|--------|
|                |     | Average             | Best   | Average   | Best   | Average | Best   |
| jacobi-1d      | 2   | 596                 | 596    | 646       | 472    | 682     | 660    |
|                | 4   | 1493                | 1492   | 1617      | 1272   | 1789    | 1756   |
|                | 8   | 3136                | 3136   | 2845      | 2560   | 3431    | 3216   |
|                | 16  | 6340                | 6338   | 4519      | 3841   | 5089    | 4872   |
|                | 32  | 8923                | 8750   | 6742      | 6026   | 6883    | 6634   |
| jacobi-2d      | 2   | 2994                | 2991   | 4327      | 4002   | 3445    | 3342   |
|                | 4   | 5701                | 5700   | 8405      | 7379   | 7370    | 7247   |
|                | 8   | 9417                | 9416   | 14872     | 13802  | 13168   | 12895  |
|                | 16  | 16274               | 16231  | 22626     | 21625  | 21565   | 21098  |
|                | 32  | 22181               | 21758  | 30423     | 28911  | 29558   | 28979  |
| lu             | 2   | 5210                | 5162   | 5351      | 4160   | 6085    | 6039   |
|                | 4   | 13528               | 13510  | 21258     | 13141  | 22979   | 16959  |
|                | 8   | 33307               | 33211  | 53643     | 44342  | 57437   | 49080  |
|                | 16  | 74543               | 74006  | 105289    | 96617  | 108189  | 102868 |
|                | 32  | 130674              | 129954 | 156187    | 147852 | 164737  | 158621 |
| ludcmp         | 2   | 5380                | 5337   | 5731      | 5337   | 6942    | 5339   |
|                | 4   | 14744               | 14744  | 25247     | 19339  | 22368   | 22065  |
|                | 8   | 37228               | 37069  | 60298     | 50208  | 60255   | 50101  |
|                | 16  | 78646               | 78467  | 106223    | 98324  | 109920  | 99798  |
|                | 32  | 134758              | 134288 | 158619    | 151063 | 165018  | 155120 |
| mvt            | 2   | 24528               | 23091  | 57216     | 33263  | 21281   | 19792  |
|                | 4   | 74386               | 73035  | 55679     | 36564  | 38215   | 35788  |
|                | 8   | 86525               | 82221  | 62453     | 47771  | 46776   | 43724  |
|                | 16  | 99144               | 97941  | 71650     | 59399  | 54925   | 48385  |
|                | 32  | 105066              | 104917 | 83635     | 79030  | 62584   | 60389  |
| seidel-2d      | 2   | 4991                | 4969   | 4374      | 3401   | 4772    | 4638   |
|                | 4   | 12197               | 12169  | 13177     | 12553  | 11784   | 11485  |
|                | 8   | 21419               | 21400  | 24396     | 22452  | 21937   | 21619  |
|                | 16  | 38222               | 38110  | 38065     | 35777  | 39747   | 38831  |
|                | 32  | 52246               | 51531  | 58319     | 57012  | 59278   | 57885  |
| symm           | 2   | 94357               | 94214  | 26374     | 24629  | 43597   | 43330  |
|                | 4   | 127497              | 126207 | 59815     | 49450  | 85730   | 78379  |
|                | 8   | 152984              | 151168 | 91892     | 75126  | 118259  | 111126 |
|                | 16  | 167822              | 167512 | 105418    | 96322  | 135278  | 131127 |
|                | 32  | 174938              | 174843 | 108950    | 99584  | 145903  | 141223 |
| syr2k          | 2   | 11098               | 3894   | 4343      | 900    | 16124   | 14404  |
|                | 4   | 49662               | 48021  | 12192     | 3121   | 22915   | 17959  |
|                | 8   | 57584               | 57408  | 29194     | 24912  | 28787   | 27259  |
|                | 16  | 59780               | 59594  | 29519     | 26327  | 31807   | 29132  |
|                | 32  | 60502               | 60085  | 36111     | 34079  | 36689   | 35155  |
| syrk           | 2   | 219263              | 218019 | 76767     | 3240   | 11740   | 9036   |
|                | 4   | 289509              | 289088 | 72148     | 9995   | 56832   | 34893  |
|                | 8   | 329466              | 327712 | 112236    | 66981  | 121664  | 109730 |
|                | 16  | 354223              | 351824 | 179042    | 172076 | 184437  | 170781 |
|                | 32  | 362016              | 359544 | 196173    | 186162 | 224330  | 213676 |
| trisolv        | 2   | 6788                | 3549   | 367       | 280    | 336     | 336    |
|                | 4   | 43927               | 43549  | 38148     | 1277   | 828     | 828    |
|                | 8   | 66148               | 65662  | 20163     | 9364   | 2156    | 2156   |
|                | 16  | 71838               | 71447  | 20421     | 12847  | 6240    | 5881   |
|                | 32  | 79125               | 79071  | 25279     | 19949  | 13431   | 13172  |
| trmm           | 2   | 138937              | 138725 | 50057     | 32720  | 13659   | 3440   |
|                | 4   | 192752              | 191492 | 58477     | 16617  | 72276   | 35000  |
|                | 8   | 225192              | 223529 | 92185     | 58957  | 134574  | 102693 |
|                | 16  | 240788              | 238159 | 128838    | 122111 | 157277  | 145934 |
|                | 32  | 246407              | 245173 | 153644    | 147551 | 171562  | 158113 |
| <b>Geomean</b> |     | 1.00                | 0.96   | 0.74      | 0.50   | 0.63    | 0.57   |

Table A.2: Comparing the edge cuts obtained by CoHyb\_CIP and CoTop with those obtained by the evolutionary algorithm of Moreira et al. on the Polyhedral Benchmark Suite (second set of results). The last line (Geomean) is for the whole PolyBench dataset (i.e., computed by combining this table with the previous one), where the performance of the algorithms are normalized with respect to the average values shown under the column Moreira et al.

| Graph      | k  | CoHyb_CIP |       | CoTop   |       |
|------------|----|-----------|-------|---------|-------|
|            |    | Average   | Best  | Average | Best  |
| 2mm        | 2  | 1.001     | 1.001 | 1.001   | 1.001 |
|            | 4  | 1.028     | 1.030 | 1.024   | 1.001 |
|            | 8  | 1.030     | 1.030 | 1.030   | 1.030 |
|            | 16 | 1.029     | 1.030 | 1.030   | 1.030 |
|            | 32 | 1.030     | 1.030 | 1.030   | 1.030 |
| 3mm        | 2  | 1.021     | 1.009 | 1.017   | 1.017 |
|            | 4  | 1.027     | 1.030 | 1.030   | 1.030 |
|            | 8  | 1.030     | 1.030 | 1.030   | 1.030 |
|            | 16 | 1.030     | 1.030 | 1.030   | 1.030 |
|            | 32 | 1.030     | 1.030 | 1.030   | 1.030 |
| adi        | 2  | 1.000     | 1.000 | 1.030   | 1.030 |
|            | 4  | 1.030     | 1.030 | 1.030   | 1.029 |
|            | 8  | 1.030     | 1.030 | 1.030   | 1.030 |
|            | 16 | 1.030     | 1.030 | 1.030   | 1.030 |
|            | 32 | 1.030     | 1.030 | 1.030   | 1.030 |
| atax       | 2  | 1.010     | 1.011 | 1.030   | 1.030 |
|            | 4  | 1.020     | 1.030 | 1.030   | 1.030 |
|            | 8  | 1.027     | 1.016 | 1.029   | 1.030 |
|            | 16 | 1.029     | 1.030 | 1.030   | 1.030 |
|            | 32 | 1.030     | 1.030 | 1.030   | 1.030 |
| covariance | 2  | 1.022     | 1.023 | 1.030   | 1.030 |
|            | 4  | 1.026     | 1.021 | 1.030   | 1.030 |
|            | 8  | 1.028     | 1.030 | 1.030   | 1.030 |
|            | 16 | 1.029     | 1.030 | 1.030   | 1.030 |
|            | 32 | 1.030     | 1.030 | 1.030   | 1.030 |
| doitgen    | 2  | 1.003     | 1.000 | 1.030   | 1.030 |
|            | 4  | 1.030     | 1.030 | 1.030   | 1.030 |
|            | 8  | 1.030     | 1.030 | 1.030   | 1.030 |
|            | 16 | 1.030     | 1.030 | 1.030   | 1.030 |
|            | 32 | 1.030     | 1.030 | 1.030   | 1.030 |
| durbin     | 2  | 1.024     | 1.024 | 1.024   | 1.024 |
|            | 4  | 1.018     | 1.018 | 1.023   | 1.023 |
|            | 8  | 1.020     | 1.020 | 1.028   | 1.028 |
|            | 16 | 1.028     | 1.028 | 1.030   | 1.030 |
|            | 32 | 1.030     | 1.029 | 1.030   | 1.030 |
| fdtd-2d    | 2  | 1.007     | 1.000 | 1.006   | 1.000 |
|            | 4  | 1.023     | 1.026 | 1.021   | 1.025 |
|            | 8  | 1.026     | 1.028 | 1.027   | 1.024 |
|            | 16 | 1.027     | 1.027 | 1.029   | 1.028 |
|            | 32 | 1.029     | 1.030 | 1.028   | 1.029 |
| gemm       | 2  | 1.010     | 1.008 | 1.029   | 1.029 |
|            | 4  | 1.024     | 1.025 | 1.030   | 1.030 |
|            | 8  | 1.029     | 1.028 | 1.029   | 1.027 |
|            | 16 | 1.030     | 1.030 | 1.027   | 1.030 |
|            | 32 | 1.030     | 1.030 | 1.030   | 1.030 |
| gemver     | 2  | 1.008     | 1.000 | 1.000   | 1.000 |
|            | 4  | 1.030     | 1.030 | 1.029   | 1.030 |
|            | 8  | 1.029     | 1.025 | 1.030   | 1.029 |
|            | 16 | 1.029     | 1.029 | 1.030   | 1.030 |
|            | 32 | 1.030     | 1.030 | 1.030   | 1.030 |
| gesummv    | 2  | 1.014     | 1.010 | 1.022   | 1.022 |
|            | 4  | 1.026     | 1.013 | 1.030   | 1.030 |
|            | 8  | 1.028     | 1.027 | 1.027   | 1.030 |
|            | 16 | 1.029     | 1.029 | 1.030   | 1.030 |
|            | 32 | 1.030     | 1.030 | 1.030   | 1.030 |
| heat-3d    | 2  | 1.008     | 1.030 | 1.030   | 1.030 |
|            | 4  | 1.030     | 1.030 | 1.030   | 1.030 |
|            | 8  | 1.020     | 1.016 | 1.030   | 1.030 |
|            | 16 | 1.024     | 1.022 | 1.030   | 1.030 |
|            | 32 | 1.030     | 1.028 | 1.030   | 1.030 |

Table A.3: The partition balances for the edge cuts given in table A.1

| Graph          | k  | CoHyb_CIP |       | CoTop   |       |
|----------------|----|-----------|-------|---------|-------|
|                |    | Average   | Best  | Average | Best  |
| jacobi-1d      | 2  | 1.009     | 1.010 | 1.016   | 1.006 |
|                | 4  | 1.019     | 1.027 | 1.016   | 1.022 |
|                | 8  | 1.016     | 1.006 | 1.024   | 1.028 |
|                | 16 | 1.025     | 1.024 | 1.024   | 1.024 |
|                | 32 | 1.027     | 1.027 | 1.028   | 1.028 |
| jacobi-2d      | 2  | 1.027     | 1.030 | 1.028   | 1.030 |
|                | 4  | 1.017     | 1.012 | 1.029   | 1.030 |
|                | 8  | 1.027     | 1.027 | 1.030   | 1.030 |
|                | 16 | 1.027     | 1.028 | 1.030   | 1.030 |
|                | 32 | 1.029     | 1.028 | 1.030   | 1.030 |
| lu             | 2  | 1.023     | 1.003 | 1.030   | 1.030 |
|                | 4  | 1.027     | 1.030 | 1.029   | 1.027 |
|                | 8  | 1.030     | 1.030 | 1.030   | 1.030 |
|                | 16 | 1.030     | 1.030 | 1.030   | 1.030 |
|                | 32 | 1.030     | 1.030 | 1.030   | 1.030 |
| ludcmp         | 2  | 1.020     | 1.020 | 1.022   | 1.020 |
|                | 4  | 1.027     | 1.030 | 1.030   | 1.030 |
|                | 8  | 1.030     | 1.030 | 1.030   | 1.030 |
|                | 16 | 1.030     | 1.030 | 1.030   | 1.030 |
|                | 32 | 1.030     | 1.030 | 1.030   | 1.030 |
| mvt            | 2  | 1.020     | 1.028 | 1.024   | 1.030 |
|                | 4  | 1.021     | 1.015 | 1.028   | 1.021 |
|                | 8  | 1.025     | 1.030 | 1.029   | 1.021 |
|                | 16 | 1.028     | 1.030 | 1.029   | 1.030 |
|                | 32 | 1.029     | 1.030 | 1.030   | 1.030 |
| seidel-2d      | 2  | 1.012     | 1.011 | 1.016   | 1.008 |
|                | 4  | 1.024     | 1.022 | 1.028   | 1.025 |
|                | 8  | 1.026     | 1.030 | 1.030   | 1.030 |
|                | 16 | 1.029     | 1.029 | 1.030   | 1.030 |
|                | 32 | 1.029     | 1.028 | 1.030   | 1.030 |
| symm           | 2  | 1.016     | 1.030 | 1.030   | 1.030 |
|                | 4  | 1.021     | 1.019 | 1.030   | 1.030 |
|                | 8  | 1.027     | 1.029 | 1.030   | 1.030 |
|                | 16 | 1.030     | 1.030 | 1.030   | 1.030 |
|                | 32 | 1.030     | 1.030 | 1.030   | 1.030 |
| syr2k          | 2  | 1.018     | 1.016 | 1.026   | 1.000 |
|                | 4  | 1.029     | 1.030 | 1.020   | 1.029 |
|                | 8  | 1.030     | 1.027 | 1.029   | 1.030 |
|                | 16 | 1.030     | 1.030 | 1.027   | 1.021 |
|                | 32 | 1.030     | 1.030 | 1.030   | 1.030 |
| syrk           | 2  | 1.021     | 1.022 | 1.024   | 1.026 |
|                | 4  | 1.030     | 1.030 | 1.028   | 1.030 |
|                | 8  | 1.029     | 1.027 | 1.030   | 1.030 |
|                | 16 | 1.030     | 1.030 | 1.030   | 1.030 |
|                | 32 | 1.030     | 1.030 | 1.030   | 1.030 |
| trisolv        | 2  | 1.012     | 1.021 | 1.027   | 1.027 |
|                | 4  | 1.026     | 1.028 | 1.020   | 1.020 |
|                | 8  | 1.028     | 1.030 | 1.026   | 1.026 |
|                | 16 | 1.030     | 1.030 | 1.030   | 1.030 |
|                | 32 | 1.030     | 1.030 | 1.030   | 1.030 |
| trmm           | 2  | 1.028     | 1.024 | 1.016   | 1.010 |
|                | 4  | 1.027     | 1.021 | 1.030   | 1.030 |
|                | 8  | 1.030     | 1.030 | 1.030   | 1.030 |
|                | 16 | 1.030     | 1.030 | 1.030   | 1.030 |
|                | 32 | 1.030     | 1.030 | 1.030   | 1.030 |
| <b>Min</b>     |    | 1.000     | 1.000 | 1.000   | 1.000 |
| <b>Average</b> |    | 1.025     | 1.025 | 1.027   | 1.027 |
| <b>Max</b>     |    | 1.030     | 1.030 | 1.030   | 1.030 |

Table A.4: The partition balances for the edge cuts given in table A.2. The last 3 lines (Min, Average, Max) are for the whole PolyBench dataset (i.e., computed by combining this table with the previous one).